

UNCLASSIFIED

AD NUMBER
ADB067386
NEW LIMITATION CHANGE
TO Approved for public release, distribution unlimited
FROM Distribution authorized to U.S. Gov't. agencies only; Critical Technology; Test and Evaluation; OCT 1981. Other requests shall be referred to Air Force Avionics Laboratory, ATTN: AADO, Wright-Patterson AFB, OH 45433.
AUTHORITY
WL/IST ltr dtd 23 May 1991

THIS PAGE IS UNCLASSIFIED

ADB067386

AFWAL-TR-81-1228

UV DETECTOR MATERIALS DEVELOPMENT PROGRAM

M. Gershenzon
University of Southern California
Los Angeles, CA 90007

R.O. Engh
P.E. Petersen
Honeywell Corporate Technology Center
10701 Lyndale Ave. South
Bloomington, MN 55420

December, 1981

Final Report FOR PERIOD DECEMBER 1980 - FEBRUARY 1982

Distribution limited to U.S. Government agencies only; test and evaluation; October 1981. Other requests for this document must be referred to the Avionics Laboratory (AFWAL/AADO), Wright-Patterson AFB, OH 45433.

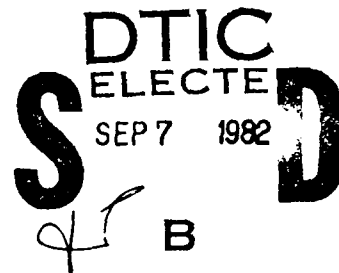
SUBJECT TO EXPORT CONTROL LAWS

This document contains information for manufacturing or using munitions of war. Export of the information contained herein, or release to foreign nationals within the United States, without first obtaining an export license, is a violation of the International Traffic-in-Arms Regulations. Such violation is subject to a penalty of up to 2 years imprisonment and a fine of \$100,000 under 22 USC 2778.

Include this notice with any reproduced portion of this document.

AVIONICS LABORATORY
Air Force Wright Aeronautical Laboratories
Air Force Systems Command
Wright-Patterson Air Force Base, Ohio 45433

82 09 07 259

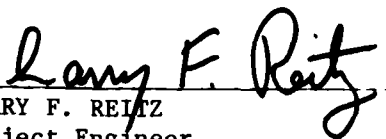


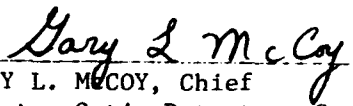
DTIC FILE COPY

NOTICE

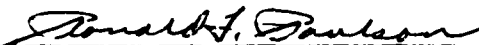
When Government drawings, specifications, or other data are used for any purpose other than in connection with a definitely related Government procurement operation, the United States Government thereby incurs no responsibility nor any obligation whatsoever; and the fact that the government may have formulated, furnished, or in any way supplied the said drawings, specifications, or other data, is not to be regarded by implication or otherwise as in any manner licensing the holder or any other person or corporation, or conveying any rights or permission to manufacture, use, or sell any patented invention that may in any way be related thereto.

This technical report has been reviewed and is approved for publication.


LARRY F. REITZ
Project Engineer
Electro-Optic Detectors Group
Avionics Laboratory


GARY L. MCCOY, Chief
Electro-Optic Detectors Group
Electro-Optics Technology Branch
Avionics Laboratory

FOR THE COMMANDER:


RONALD F. PAULSON, Chief
Electro-Optics Technology Branch
Electronic Technology Division
Avionics Laboratory

"If your address has changed, if you wish to be removed from our mailing list, or if the addressee is no longer employed by your organization please notify AFWAL/AADO-3, W-P AFB, OH 45433 to help maintain a current mailing list".

Copies of this report should not be returned unless return is required by security considerations, contractual obligations, or notice on a specific document.

UNCLASSIFIED

SECURITY CLASSIFICATION OF THIS PAGE (When Data Entered)

REPORT DOCUMENTATION PAGE		READ INSTRUCTIONS BEFORE COMPLETING FORM
1. REPORT NUMBER AFWAL-TR-81-1228	2. GOVT ACCESSION NO. AD-B667 386L	3. RECIPIENT'S CATALOG NUMBER
4. TITLE (and Subtitle) UV DETECTOR MATERIALS DEVELOPMENT PROGRAM		5. TYPE OF REPORT & PERIOD COVERED Final Report for Period December 1980-February 1982
		6. PERFORMING ORG. REPORT NUMBER 41874
7. AUTHOR(s) M. Gershenzon, R.O. Engh, P.E. Petersen		8. CONTRACT OR GRANT NUMBER(s) F33615-80-C-1106
9. PERFORMING ORGANIZATION NAME AND ADDRESS University of Southern California Los Angeles CA 90007 Honeywell Corporate Technology Center 10701 Lyndale Avenue, Bloomington MN 55420		10. PROGRAM ELEMENT, PROJECT, TASK AREA & WORK UNIT NUMBERS P.E. 62204F Project 20010397
11. CONTROLLING OFFICE NAME AND ADDRESS Avionics Laboratory (AFWAL/AADO-3) Air Force Wright Aeronautical Laboratories (AFSC) Wright-Patterson AFB Ohio 45433		12. REPORT DATE December 1981
14. MONITORING AGENCY NAME & ADDRESS (if different from Controlling Office)		13. NUMBER OF PAGES 61
		15. SECURITY CLASS. (of this report) UNCLASSIFIED
		15a. DECLASSIFICATION/DOWNGRADING SCHEDULE
16. DISTRIBUTION STATEMENT (of this Report) Distribution limited to U.S. Government agencies only; test and evaluation; October 1981. Other requests for this document must be referred to the Avionics Laboratory (AFWAL/AADO), Wright-Patterson AFB, OH 45433.		
17. DISTRIBUTION STATEMENT (of the abstract entered in Block 20, if different from Report)		
18. SUPPLEMENTARY NOTES		
19. KEY WORDS (Continue on reverse side if necessary and identify by block number) AlGa _N , UV detectors, solar blind, Schottky barriers, MO-CVD, single crystal		
20. ABSTRACT (Continue on reverse side if necessary and identify by block number) The objective of this program is to establish the feasibility of using Al _x Ga _{1-x} N as a sensor material in producing solar blind UV detectors. The Al _x Ga _{1-x} N system was selected because: 1. It has wide bandgaps which lay in the ultra violet range of energies and 2. Its spectral response can be tailored to the application by varying the aluminum to gallium ratio. There are two general problem areas in this development:		

DD FORM 1 JAN 73 1473

EDITION OF 1 NOV 65 IS OBSOLETE

UNCLASSIFIED

SECURITY CLASSIFICATION OF THIS PAGE (When Data Entered)

20. Abstract (continued)

1. The growth of single crystal $\text{Al}_x\text{Ga}_{1-x}\text{N}$ of uniform and controlled composition and
2. Evaluation and incorporation into devices.

The method selected for crystal growth was metalorganic chemical vapor deposition (MO-CVD) because:

1. It requires a lower growth temperature. Therefore, there is a lower possibility of contamination and
2. Better control of aluminum to gallium ratio is possible.

The Schottky barrier diode was selected as the device concept because it is the most direct approach to obtaining a photovoltaic effect from a material in which p-n junctions cannot be formed.

In the course of this investigation, our experiments have shown that:

- o Single crystal GaN and AlGa_N can be grown epitaxially on sapphire by MO-CVD.
- o Resistivities of as-grown GaN and $\text{Al}_x\text{Ga}_{1-x}\text{N}$ epilayers have been 1 to 2 orders of magnitude too low for Schottky barrier formation, even with Zn doping up to 10% and x-values up to .22.
- o Schottky barriers may be formed on GaN and AlGa_N epilayers after compenstion of the AlGa_N surface by acceptor ion implantation.
- o Aluminum content (x-value) controls the spectral response of Schottky barriers on ion implanted $\text{Al}_x\text{Ga}_{1-x}\text{N}$ as predicted by Vegard's Law.
- o Fabrication of UV photo diodes from $\text{Al}_x\text{Ga}_{1-x}\text{N}$ materials has been demonstrated.
- o Fabrication of detectors with peak sensitivity less than 270 nm was demonstrated.

Summary

A number of military applications, such as threat warning systems and systems employing horizon sensors, require sensitive stable ultraviolet light detectors. One of the most promising approaches to UV sensors is the development of solid-state detectors fabricated from the semiconductor AlGa_N. This material provides tunable spectral sensitivity, and offers the possibility of high peak quantum efficiency and solar blind operation.

During the 12 month span of this contract, an investigation of AlGa_N for UV detectors was undertaken. In the course of the program, single crystal AlGa_N was grown for the first time by metalorganic chemical vapor deposition (MO-CVD), a procedure was developed for producing Schottky diodes on AlGa_N, and detectors were fabricated and evaluated. The results of this initial investigation are very encouraging.

It was demonstrated that AlGa_N can be grown by MO-CVD in the compositional range required to produce detectors having peak sensitivities between 3.53 eV (351 nm) and 4.64 eV (267 nm). Detectors were fabricated which had a peak spectral response of 267 nm, as required for solar blind operation. The best detectors had an internal quantum efficiency estimated to be approximately 26 percent. A number of areas of possible improvement have been identified in the course of this work.

With the incorporation of a few specific changes in the MO-CVD growth system higher quality AlGa_N material will be available for processing into devices. A systematic investigation of this more uniform material would then produce greatly improved detectors with high UV sensitivity in the specified spectral ranges.



iii /iv

Accession For	
NTIS GRA&I	<input type="checkbox"/>
DTIC TAB	<input checked="" type="checkbox"/>
Unannounced	<input type="checkbox"/>
Justification	
By	
Distribution/	
Availability Codes	
Dist	Avail and/or Special
B	

Table of Contents

Section	Page
SUMMARY	iii
1 INTRODUCTION	1
Statement of the Problem	1
2 TECHNICAL DISCUSSION	2
3 MATERIALS AND PROCESSING	4
Materials Selection	4
Materials Status	5
Selection of Materials Parameters	8
Selection of Crystal Growth Technique	9
4 EXPERIMENTAL	11
MO-CVD GROWTH	11
Design and Construction of MO-CVD Growth System	11
Description of Growth Apparatus	13
Substrates	15
GaN Growth	15
Compensation	20
AlGaN Alloys	22
Optimized Growth Procedure	24
Discussion of Materials Preparation and Characterization	26
ELECTRICAL EVALUATION	31
Epilayer Samples	31
Transport Properties	31
Ion Implantation	32
Optical Measurements	34
5 DEVICE EVALUATION	37
Hall Measurements	37
Contacts	37
MIS Structure	41
Test Device	41
Ion Implantation	41
Optical Measurements	43
6 DISCUSSION OF RESULTS AND AREAS OF FUTURE INVESTIGATION	50
7 CONCLUSIONS	53
REFERENCES	54

List of Illustrations

Figure		Page
1	Application of Vegard's Law to the Bandgap of $\text{Al}_x\text{Ga}_{1-x}\text{N}$	8
2	Schematic Diagram of Metalorganic Chemical Vapor Deposition Epitaxy Apparatus	14
3	MO-CVD Epilayer AlGa _N No. 42 Growth on Sapphire Substrate. (Mag. 3.75X)	16
4	AlGa _N No. 42 Showing Step Growth and Hexagonal Symmetry Defect. (SEM 10,000X)	19
5	Cleaved Cross Section of AlGa _N No. 45. 4.5 μm of AlGa _N on 11 μm of Ga _N on Basal Sapphire Substrate. (SEM 2,200X)	19
6	Planar Surface of Ga _N No. 23 on Basal Plane Sapphire. (SEM 20,000X)	23
7	Cross Section of Cleaved Sample Ga _N 35.	32
8	Honeywell's Computerized Materials Evaluation Facility	33
9	Instrumentation for Optical Measurements	35
10	Carrier Concentration, and Mobility as a Function of Temperature for Ga _N Epilayer	39
11	I-V Curves of Ohmic Contacts on AlGa _N No. 43, Indium to Indium (a) and Tin to Tin (b)	40
12	Gold Schottky Contacts 1mm in Diameter on Sample Ga _N 35	40
13	AlGa _N Test Device Showing Two Ohmic Contacts and Two Schottky Barrier Contacts	42
14	Implanted Beryllium Density Profile, Calculated from LSS Theory	42
15	I-V Curves of Ga _N and AlGa _N , Unimplanted and Implanted with Be	44
16	Transient Response of AlGa _N 43	45
17	Spectral Response Curve of Implanted Ga _N Epilayer	45
18	Spectral Response Curve of Implanted AlGa _N Epilayer (AlGa _N 43, $x = 0.042 \rightarrow 0.068$)	46
19	Spectral Response Curve of Implanted AlGa _N Epilayer (AlGa _N 42, $x = 0.112 \rightarrow 0.224$, not single crystal)	46

Section 1 Introduction

STATEMENT OF THE PROBLEM

To achieve a solid-state solar blind UV detector, two major problems must be solved. First a technique for growing $\text{Al}_x\text{Ga}_{1-x}\text{N}$ of controlled composition (x-value) and carrier concentration must be developed. Although AlGa_N has been successfully grown over the entire range of composition, no laboratory has successfully controlled the carrier concentration in the range required for Schottky barrier formation. Our approach is to develop a new technique, metalorganic chemical vapor deposition (MO-CVD) for growing the AlGa_N. As will be discussed in detail below, MO-CVD is a lower temperature growth process and utilizes less corrosive materials than other CVD processes. Hence, the prospects for achieving higher purity (lower carrier concentration) are much greater using the process than with the previously explored processes.

The second major problem is developing the technology for Schottky barrier detectors. Since AlGa_N has not been widely exploited for device applications, the device processing technology is not well developed. This program is the first to investigate Schottky barrier formation on AlGa_N. Both the development of a controlled AlGa_N growth process and Schottky barrier technology have been addressed in this program.

Section 2

Technical Discussion

Threat warning systems and systems requiring horizon sensors both need photodetectors operating in two distinct wavelength ranges in the ultraviolet region of the spectrum. In these detectors the wavelength rejection ratios are important, that is, detectivity should increase from near zero to its peak in a very short wavelength span. Thus the detector material should be a semiconductor in which bandgap absorption sets in very abruptly. For the absorbed photons to be detected electrically, the electrons and holes produced must be separated before they recombine. This is most conveniently accomplished by drift in a high electric field. The extremely high voltages that would be necessary to establish a suitably high field in a bulk semiconductor layer, or the precision in grown layer thickness necessary to avoid such high voltages, argues for a narrow, high field region determined by a built-in barrier and augmented, if desired, by an externally applied bias. For semiconductors this means either a p-n junction, a heterojunction or a Schottky barrier. In materials whose band gaps fall in the ultraviolet, the heats of formation of native defect donors and acceptors, usually vacancies, are generally lower than the electrical compensation energies gained. Therefore, such materials only exist in n-type form or p-type form, but not both. Usually they are n-type. Thus p-n junctions are not possible in these high bandgap semiconductors. Heterojunctions depend on a materials compatibility between the semiconductor of interest and a lower bandgap semiconductor. We will show that such a possibility does indeed exist for one of the wavelength regions considered, but not easily for both regions. Hence, a Schottky barrier emerges as the device configuration most likely to prove viable with the least amount of effort.

Within the constraints of the Schottky barrier approach, four guidelines are immediately apparent for selecting the semiconductor material and its eventual device structure. First, since two wavelength regions are required, it is highly desirable that they both be feasible in the same semiconductor materials system. It will be shown below that the optimum system is $\text{Al}_x\text{Ga}_{1-x}\text{N}$. Second, the dominant semiconductor parameter to be chosen is the bandgap to match the two required wavelength regions. Both bandgaps can be chosen within the $\text{Al}_x\text{Ga}_{1-x}\text{N}$ system. Third, the metal-semiconductor junction must result in a depletion region in the semiconductor in which the photogenerated electrons and holes are separated by the built-in electric field, augmented, if desirable, by an externally applied bias. No electron affinity measurements have been made on the AlN-

GaN system. All that can be said at present is that matching between these semiconductors and high work function metals (Au,Pt) will occur in the upper half of the bandgap. Fourth, the doping of the semiconductor is crucial. If the material is too heavily doped n-type ($\sim 10^{18}\text{cm}^{-3}$), the depletion layer will be very narrow, and tunneling of electrons from the metal to the semiconductor through the Schottky barrier will lead to leakage current, or in the high doping limit, to a low resistance contact rather than to a good blocking Schottky barrier contact. If the uncompensated doping is too low, that is if the Fermi level lies greater than several kT below the conduction band, the bulk material, beyond the depletion layer will be highly resistive. While this effect could be minimized by careful control of the active layer thickness, it would be far simpler to control the Fermi level position itself, so that the bulk resistivity is sufficiently low to avoid a high series resistance, yet sufficiently high to produce a wide depletion layer that inhibits tunneling. In the AlN-GaN system, this prescribes a net shallow donor concentration range of 10^{16} to 10^{17}cm^{-3} .

Section 3 Materials and Processing

MATERIALS SELECTION

The detector material must be a semiconductor, not a metal or a semimetal, or a highly resistive ionic crystal whose Fermi level is essentially uncontrollable. Four considerations for the choice of the specific semiconductor system have been noted above: the system should permit implementation of both required wavelength ranges, the bandgap can be adjusted to match the appropriate ranges, appropriate Schottky barriers are feasible, and sufficient Fermi level control is possible to avoid barrier tunneling and to avoid high series resistance.

Group IV semiconductors were ruled out because the required wavelength cannot be matched. The bandgap of Si is too low, that of diamond too high. C and Si are immiscible in the solid state, except for the discrete compound SiC whose bandgap is too low. Group II-VI semiconductors can also be eliminated. IIB-VIA compounds between Zn, Cd and O,S,Se,Te have bandgaps which do not meet both wavelength ranges requirements. Of these, only ZnS can meet one of these, the longer wavelength. However, there is no alloy to increase its bandgap. That of ZnO is smaller. Furthermore, planar single crystal growth of ZnS is not trivial. Of the IIA-VIA compounds, most of these, involving Ca, Sr, Be are clearly ionic, and hence unsuitable. Those involving Be and Mg with O,S,Se or Te are possibilities. The oxides are not wurtzite structures and are immiscible with the others and, therefore, are ruled out. The remainder are highly ionic semiconductors in which miscibility and Fermi level control possibilities have received little attention in the literature. Hence a major materials development program would be a necessary prerequisite to determine if any of these materials or their alloys would be suitable. Such a long range program is not matched to the constraints of this contract. Furthermore, these materials tend to oxidize in air and especially in moist air, so that additional fabrication and passivation control would become necessary. Thus, we ruled out all II-VI compounds.

The more exotic semiconductors were eliminated because, either their bandgaps are too small—the IV-VI compounds, most of the chalcopyrites—or because the wider bandgap materials of the chalcopyrite ternaries or the II-IV compounds (for example, Mg_2Si) behave more like the very ionic II-VI materials in which there is not yet a reasonably well

established growth technology. Also, either the compounds are unstable under ambient conditions, or little is known of their solid-state miscibilities for matching their bandgaps to the required wavelength ranges.

Finally, we considered the III-V compounds. Of the phosphides, arsenides and antimonides of Al, Ga and In, none have sufficiently high bandgaps. The boron compounds do, but these have different crystal structures, are immiscible with the standard III-V compounds, and can only be grown at extremely high temperatures and pressures. Hence we are left with the Group III nitrides. AlN, GaN and InN are completely miscible among each other, but they are of wurtzite structure and are immiscible with the more conventional III-V zincblende compounds. The attainable bandgaps range from 1.4 for InN to about 5.1 eV for AlN, thus completely covering the wavelengths required for this program. In fact, GaN itself falls within one of the ranges, 0.35 - 0.42 microns. The second range, of shorter wavelength, corresponds to an $\text{Al}_x\text{Ga}_{1-x}\text{N}$ crystal range of $0.3 < x < 0.8$. Thus, InN is not required. Furthermore, the technology of GaN and AlN is moderately well advanced and in recent years, progress has been made on the growth and physical properties of their ternary alloys. Finally both GaN, AlN and their alloys are stable in moist air. Thus, we opt for the $\text{Al}_x\text{Ga}_{1-x}\text{N}$ system to fulfill the materials requirements of a solid state solar blind UV detector.

MATERIALS STATUS

The University of Southern California has had a program on the preparation and properties of GaN for over 10 years. The original goal of the project was to develop ultraviolet p-n junction LEDs and lasers, but low resistivity p-type material has so far been impossible to achieve. Several years ago the Office of Naval Research began supporting USC to investigate GaN as a possible fast, high power material for transit time-limited microwave devices.

The current status of GaN will be briefly summarized here, based on our work^{1,2} as well as that of Illegems at Bell Labs³, Pankove at RCA⁴ Madar and Jacob in France⁵⁻¹⁰, Wickenden in England¹¹, and some Soviet work^{12,13}. Neither Bell Labs nor RCA are currently working on GaN.

GaN is a wide, direct gap (3.4 eV 3700Å), fairly ionic wurtzite structure semiconductor. Its estimated melting point is 3400°C with an equilibrium N_2 pressure of 100,000 atm. Even at 1000°C, its N_2 decomposition pressure is about 100 atm. It is grown by nonequilibrium growth from an active nitrogen source, NH_3 . At 1000°C, NH_3 should

almost completely dissociate into N_2 and H_2 . To obtain 100 atm of N_2 at $1000^\circ C$ from NH_3 , only about 5 torr of NH_3 would be left undissociated. Yet the homogenous kinetics of this reduction are very slow. Below $1100^\circ C$, GaN can be grown by a vapor phase reaction between a Ga-containing species, a halide or a metalorganic compound, and NH_3 of at least 5 torr pressure, because the rate of formation of GaN can be made greater than its decomposition into Ga and N_2 .

No semiconductor substrate, except ZnO (which is incompatible with the presence of HCl in halide transport of Ga), offers a good lattice match, but sapphire has been found to be a suitable substrate. The solubility of NH_3 in liquid Ga is infinitesimal¹⁴, so that liquid phase epitaxy is not appropriate. Hence we have used a halide transport method ($HCl + GaCl$), reacting the halide with NH_3 over a sapphire substrate.

1 M. Gershenzon, Annual Technical Progress Report, "Evaluation of Gallium Nitride for Active Microwave Devices," ONR N00014-75-C-0295, Sept. 1978 (AD A064299).

2 M. Gershenzon, Annual Technical Progress Report, "Evaluation of Gallium Nitride for Active Microwave Devices," ONR N00014-75-C-0295, Sept. 1979 (AD A079319).

3 M. Illegems and H.C. Montgomery, J. Phys. Chem Solids 34, 885 (1973).

4 J.I. Pankove, J.E. Berkeyheiser and E.A. Miller, J. Appl. Phys. 45, 1280 (1974) (and reference appended).

5 G. Jacob, R. Madar and J. Hallais, Mater. Res. Bull. 11, 445 (1976).

6 R. Madar, G. Jacob, J. Hallais and R. Fruchart, J. Cryst. Growth 31, 197 (1975).

7 G. Jacob, Acta Electron. 21, 159 (1978).

8 G. Jacob, M. Boulow and M. Furtado, J. Cryst. Growth 42, 136 (1977).

9 R. Madar, D. Michel, G. Jacob and M. Boulow, J. Cryst. Growth 40, 239 (1977).

10 G. Jacob, M. Boulow, M. Furtado and D. Bois, J. Electron. Mater. 7, 499 (1978).

11 J. Hagen, R.D. Metcalfe, D. Wickenden and W. Clark, J. Phys. C. 11, L143 (1978).

12 B. Baranov and L. Daeweritz, Phys. Status SolidiA 38, K111 (1976).

13 B. Baranov, L. Daeweritz, V.B. Gutan, G. Jungk, H. Neumann and H. Raidt, Phys. Status SolidiA 49, 629 (1978).

14 R.A. Logan and C.D. Thurmond, J. Electrochem. Soc. 119, 1727 (1972).

Like GaN, AlN is a very refractory material (estimated melting point 3400°C at a N_2 pressure of 10^5 atm.). Most work on AlN has been done behind the Iron Curtain and the grown crystals have not been subjected to the same detailed optical examination as for GaN. Hence the bandgap is known only approximately (5.25 to 6.2 eV) and, like GaN, it is probably direct. It is usually grown from the vapor phase, either as small non-epitaxial crystallites or epitaxially on sapphire. Unlike GaN, as-grown crystals are always high-resistivity, although they can be doped to produce low-resistivity n-type crystals. Although most vapor phase growth uses the halide ($AlCl_3$) reaction with NH_3 as for GaN, Dr. K. Lakin at USC grew AlN epitaxially on sapphire for surface acoustic wave devices using a metalorganic vapor source $[(CH_3)_3Al]$ for Al in a silicon-silane type reactor.

Although the covalent radii of Ga and Al are almost identical, leading to unrestricted epitaxy of alloys in the AlAs-GaAs system, the nitrides are fairly ionic. Hence the lattice constants of GaN and AlN differ somewhat in their respective wurtzite structures. For GaN, $a = 3.180\text{\AA}$ and $c = 5.166$; for AlN, $a = 3.104$ and $c = 4.965$, differences of 2.5 percent and 4 percent in a and c , respectively.

Recently, two papers reported that AlN and GaN are miscible in solid solution over the entire composition range. The first paper was by a group in England¹¹ the second by a group in East Germany and the Soviet Union^{12,13}. Both used the halide transport method to react $AlCl_3$ and $GaCl$ (the former passing HCl over a single boat containing Ga and the Al) with NH_3 on a sapphire substrate at $\sim 1050^\circ C$ in a N_2 carrier gas ambient. The English group used absorption (above a level of $3 \times 10^4 \text{ cm}^{-1}$) to show that the edge was direct over the entire alloy range. (At lower absorption levels an apparent Urbach tail obscures the nature of the edge.) Edge luminescence follows the optical absorption edge, and deviations from a linear Vegard's Law bandgap composition relationship are not pronounced. The East German group went only to 45 percent Al. They observed that the high electron density characteristic of their GaN (10^{19} cm^{-3}) persisted in all their alloys, although it tended to decrease with Al incorporation. However, they reported that chemical analyses showed a Si concentration of 1.5 percent ($10^{21}/\text{cm}^{-3}$), and we knew that Si is a shallow donor.

Both Pankove at RCA and our group at USC have ion-implanted Al in GaN crystals. We both observed a shift of all luminescence bands to higher energies consistent with a linear composition dependence of the bandgap up to about 10 percent Al.

SELECTION OF MATERIALS PARAMETERS

In selecting the materials composition in the $\text{Al}_x\text{Ga}_{1-x}\text{N}$ system it is necessary to match two prescribed wavelength regions. For the given long wavelength regime, 0.35 to 0.42 micron, GaN itself, with a bandgap of 3.4 eV corresponding to 0.365 micron was ideally suited. The short wavelength specification, 0.24 to 0.29 micron corresponds to a bandgap range of 4.3 to 5.2 eV. The composition of the $\text{Al}_x\text{Ga}_{1-x}\text{N}$ required to respond in the two specified wavelength regions can be calculated assuming the validity of Vegard's Law, which linearly relates the bandgap of a compound to its composition. Figure 1 is a graph of the application of Vegard's Law to the bandgap of the $\text{Al}_x\text{Ga}_{1-x}\text{N}$ system.

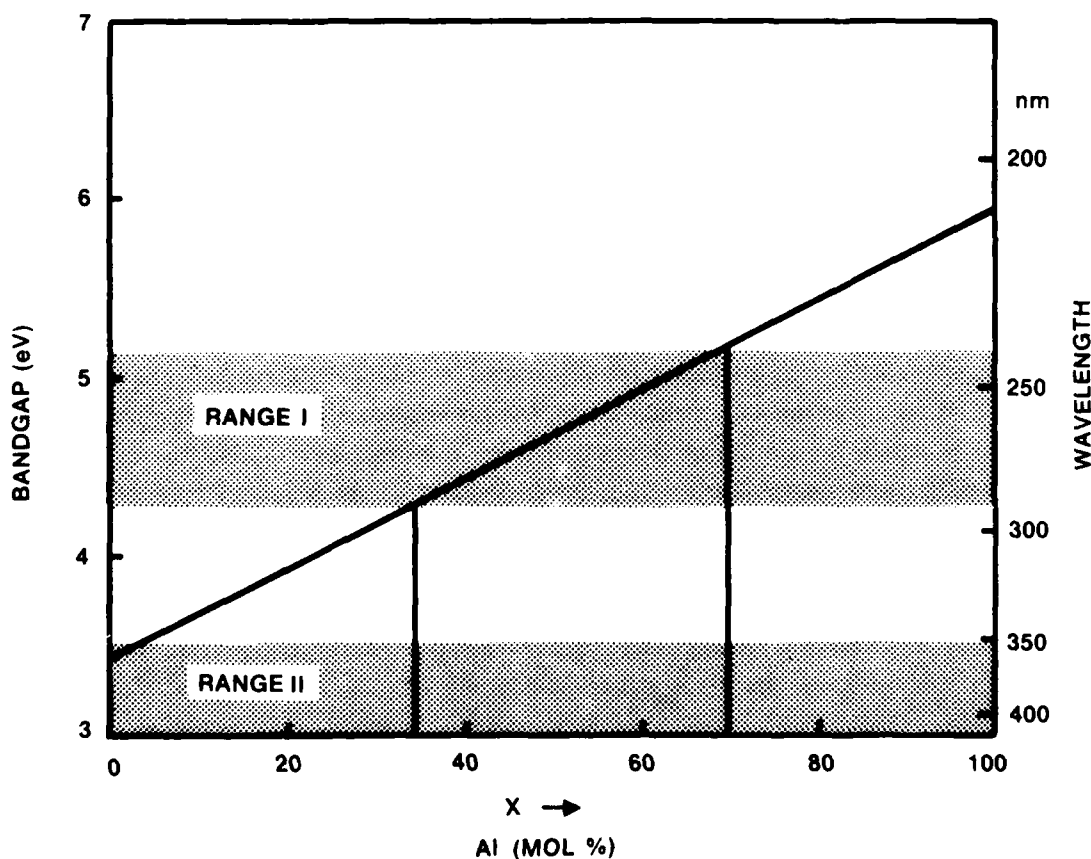


Figure 1. Application of Vegard's Law to the Bandgap of $\text{Al}_x\text{Ga}_{1-x}\text{N}$

SELECTION OF CRYSTAL GROWTH TECHNIQUE

It has already been concluded that GaN and $\text{Al}_x\text{Ga}_{1-x}\text{N}$ are the materials of choice to match the two desired cut-off wavelengths. Single crystal material is required for good Schottky barriers because grain boundaries can cause high leakage currents or exhibit high resistance. The melt growth of these alloys is ruled out because the melting point and equilibrium N_2 pressures are much too high, as noted above. Furthermore, the N_2 pressure required for LPE growth (200-500 atm at 1200°) is also too high. Thus, a non-equilibrium source of nitrogen, NH_3 , is substituted for N_2 . NH_3 decomposes slowly at 1100°C . The solubility of NH_3 in Ga is too low for LPE growth even at 1100°C . Hence growth must be by a vapor technique. Attempts to grow GaN by reactive evaporation or sputtering using a plasma or glow discharge in N_2 or NH_3 always lead to polycrystalline material (at substrate temperatures below 600°C).

Two vapor growth techniques, therefore, became the logical candidates for our selection. The first was the halide-hydride VPE method in which GaCl is reacted with NH_3 in a hot wall reactor. The second was the MO-CVD method where $(\text{CH}_3)_3\text{Ga}$ is reacted with NH_3 in a cold wall reactor. Most of our previous growth experience with GaN has been with the VPE technique. However, for this study we opted for the MO-CVD method for several reasons. First, for the AlGaIn alloys, the control of the Al:Ga ratio would be very difficult with the halide process because the Al would tend to come off preferentially for an Al-Ga mixture in a single boat; thus, the first growth would be Al-rich and later, when the Al is depleted the layers would become Ga-rich. Hence two separate chambers would be needed, one for a Ga boat and the other for an Al boat. For MO-CVD growth, the Al:Ga ratio should be determined completely by the injected streams of the two metalorganic sources; hence, it is simply controlled by flow rates. Second, Al and AlCl_3 are very reactive at high temperatures. The VPE technique requires a hot wall. Even in our VPE growth of GaN, it was necessary to line the hot fused silica growth tube with an alumina liner to avoid contact of the reactant gases with the hot SiO_2 . Failure to do so resulted in the incorporation of up to 10^{21} cm^{-3} shallow Si donors in the grown GaN. Aluminum is even more reactive than gallium. In MO-CVD growth the outer walls remain cold and unreactive. Third, it was anticipated that the crystals would have to be compensated during growth (at least for the GaN material). In VPE, this requires an extra hot chamber with its own gas flow and temperature control to transport the compensating element such as Zn, in a controlled manner. In MO-CVD growth the incorporation of an element such as Zn is easily controlled via the flow rate of a metalorganic compound, for example $(\text{C}_2\text{H}_5)_2\text{Zn}$. Fourth, the lowest temperature at which single crystal growth occurs in MO-CVD depends only on the kinetics on the growing

interface and not on the thermodynamics of the reacting species. The interface limit is the lower limit for both MO-CVD and halide-hydride VPE growth, but the latter usually requires higher temperatures to drive the reaction to near completion. Hence, MO-CVD growth should involve the lowest possible temperatures, presumably reducing the impurity incorporation problem. Fifth, the growth of single crystals of both GaN and AlN by MO-CVD had already been demonstrated.

Section 4

Experimental

MO-CVD GROWTH

Design and Construction of MO-CVD Growth System

Since the desired range of AlGaIn materials had never been grown by MO-CVD, the growth parameters were not known, and since it was not clear at the outset whether in situ compensation or substrate cleaning would be necessary, the system was designed to be as flexible as possible. This meant a simple design without many of the useful, but constraining features of a growth system based upon a well-developed technology.

A vertical fused silica reactor configuration was selected because flow patterns in such a system are easier to diagnose and alter than with a horizontal geometry. At the outset, it was not known whether $(\text{CH}_3)_3\text{Ga}$ and NH_3 would form a low temperature addition compound, as they do in the Al-N system and in some other semiconductor systems, for example, $(\text{CH}_3)_3\text{In}$ and PH_3 . If an additional compound forms, as it did, resulting in small particles settling on the reactor walls and on the substrate, single crystal growth would be impossible. Thus the reactor was designed to allow, as options, both the metalorganic vapor and the NH_3 to mix well before impinging on the substrate, and provision for keeping the two species apart until they reached the substrate. In addition, the reactor was designed for possible use at reduced pressures, although this option was never exploited. Lower pressures reduce the stagnant gas layer at the growing interface, increasing the diffusion of reactants to the interface and of by-products away from the interface. Lower pressures also increase the linear flow rate across the interface, simplifying the flow patterns, and reduce the probability of forming addition compounds via the law of mass action. In the present system, the mechanical roughing pump incorporated to do this was only used for purging and for leak-testing the manifold. Finally, a separate inlet was installed to provide a sheath of laminar flowing gas to separate the inner reactant stream from the quartz envelope. In addition to providing isolation by an inert gas, this path could also be used for the NH_3 or for the HCl , the latter either for cleaning the substrate surface or for converting the metalorganic vapor to a halide. This provision also was not necessary.

Substrate heating in this vertical reactor design was by conduction from a graphite susceptor heated by a radio frequency (RF) source. The temperature of the growing

interface was measured either by an optical pyrometer, (one color temperature) taking account of the emissivity of the surface, or by a thermocouple in an inner quartz tube extending to the susceptor pedestal, but separated from it by a quartz wall. The pedestal-thermocouple assembly is part of a simple exhaust system below the growth area, easily disassembled by an O-ring sealed standard taper joint for rapid dismounting when changing samples. A more complex pedestal mount was designed, but never built, in which the thermocouple penetrated the graphite susceptor for better temperature measurement.

The manifold was also designed for flexibility and simplicity. Stainless steel tubing with "Swagelok" type connectors (double ferrules, no teflon or pipe dopant sealants) was used throughout the system except for the simple glass rotameter (floating sapphire ball) flowmeters. Two mass flowmeters, with servo-actuated control valves and associated circuitry were ordered for the system as soon as the contract funds were available. They were chosen to control the metalorganic Ga and Al streams to provide good alloy composition control for the AlGa_N crystals. However, by the time they were delivered, the contract period was almost over. Hence they were never installed. In addition, a Johnson-Matthey Pd-diffuser H₂ purifier was also ordered at the same time. Again, the unit arrived late in the contract period, and because H₂ purity was noted not to be a critical parameter at the time, this also was not installed, again as for the mass flowmeters, to avoid down-time. Here the use of electronic grade H₂ with H₂O traps proved sufficient.

At the outset it was not clear whether the reactants chosen [(CH₃)₃Ga, (CH₃)₃Al and NH₃] were optimum choices. A switch to (C₂H₅)₃Ga and (C₂H₅)₃Al might be useful to reduce the formation of addition compounds with NH₃. Thus provisions were made for the use of temperature controlled water for ice baths, both below and above room temperature for the metalorganic sources, and for a wide flow control range of H₂ through the metalorganic bubblers. In addition, extra inlet lines were provided for doping during growth [(C₂H₅)₂Zn was eventually used] and for cleaning (HCl, never needed) and purging (H₂, N₂) lines.

Before experiments began, the newly assembled system was tested for leaks by the integral pumping system (mechanical roughing pump, thermocouple gauge and associated valves). The susceptor thermocouple was calibrated against the graphite susceptor surface temperature by the observation of melting of known melting point metals on the graphite surface and against substrate surface by the optical pyrometer.

Here, both sapphire and GaN were used as well as direct observations of the graphite susceptor.

Description of Growth Apparatus

A schematic diagram of the metalorganic vapor-phase epitaxy apparatus is shown in Figure 2. The vertical growth reactor was made of quartz tubing 55 cm long and 50 mm ID. The susceptor, machined from high-purity graphite obtained from Ultra Carbon Corporation, was heated inductively via a four-turn coil by a RF source. It was one inch in diameter at its widest and accommodated sapphire substrates up to one inch in diameter. The exhaust (bottom) of the growth reactor was detachable from the top portion to facilitate substrate loading and unloading of the grown specimen. The two ends of the growth reactor were clamped to one another through O-ring joint connectors. A quartz tube of 11mm OD extended upwards from the detachable bottom end of the growth reactor and served as a support for the susceptor. The gas inlet lines connect to the top portion of the reactor while the exhaust line connects to the bottom part. Gas lines were constructed of stainless steel tubing using Swagelok tube fittings.

The flow rates of the various gases admitted into the growth reactor were metered and monitored respectively by needle valves and flow meters, both purchased from Matheson Gas Products. H_2 was used as the carrier gas for trimethylgallium (TMG), diethylzinc (DEZ), trimethylaluminum (TMA). Electronic grade ammonia with a stated purity of 99.999 percent was obtained from Airco Inc.

The metalorganics, TMG, DEZ, and TMA were purchased from the Alfa Division of the Ventron Corporation and had stated purities of 99.9995 percent. The metalorganics were kept in a liquid state inside separate stainless steel bubblers. The TMG bubbler was maintained in an ice-filled dewar during growth runs, but DEZ and TMA were kept at room temperature. The saturated vapor pressure of the three metalorganics are known at the appropriate temperatures. Thus, known quantities of each metalorganic can be transported into the growth reactor by bubbling metered amounts of H_2 through the liquid.

A rotary mechanical pump was connected to the whole system to facilitate leak-checking. Considerable effort was spent to ensure that the entire system was as leak-free as possible at joints and fittings. This is most important since the metalorganics used have a great affinity for O_2 and also are highly toxic. The pressure of the evacuated system was measured using a thermocouple vacuum gauge and a NRC 741 gauge control.

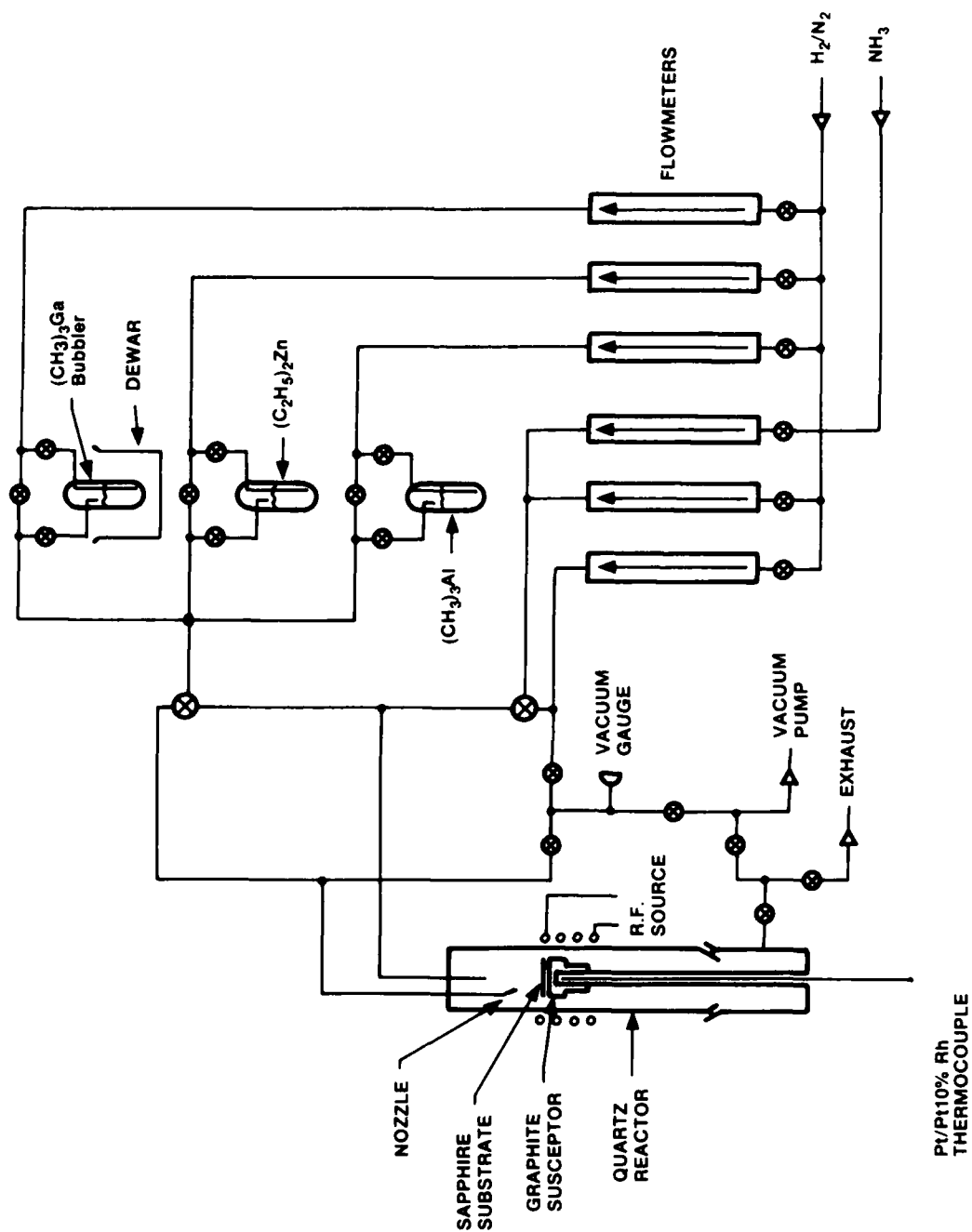


Figure 2. Schematic Diagram of Metalorganic Chemical Vapor Deposition Epitaxy Apparatus

The susceptor temperature was monitored by a Pt-Pt/10 percent Rh thermocouple inserted into its base through the 11 mm quartz support tube.

Substrates

As noted in the original proposal, it was intended to grow the GaN and AlGaIn on basal plane sapphire substrates. Alternatively, we would grow on GaN epitaxial layers (on basal plane sapphire) already prepared by an existing halide-hydride (GaCl-NH_3) VPE system. From our previous work with GaN on the VPE system^{15,16}, it was known that planar morphology could be obtained on basal plane sapphire but not on the more commonly available (and five times cheaper) R-plane sapphire (the latter commonly used for SOS silicon). The supplier of sapphire could not promise us delivery of basal plane material for at least three months. Thus, knowing full well that planar morphology would not occur, we began with R-plane substrates. When the basal plane substrates finally appeared, we faced another problem. Sometimes good planar epilayers of GaN or AlGaIn would grow; sometimes only whiskers and very thin polycrystalline layers would appear. We discovered the problem was that many of the so-called basal plane substrates shipped were not really basal plane orientation. Planar GaN and AlGaIn grew only on the basal plane orientation. It then became vital to check the Bragg X-ray diffraction on every substrate received, looking for the basal plane reflection, before attempting growth. The supplier was unwilling to believe that they were shipping us incorrectly oriented substrates. Again, time elapsed as sapphire material had to be replaced.

The good substrates were received polished on only one side. These were cut into 1 x 2 cm pieces by diamond saw. The substrates were then cleaned by (1) organic cleaning (benzene, trichlorethylene, methyl alcohol, water), (2) lightly etched ($\text{H}_3\text{PO}_4\text{:H}_2\text{SO}_4$; 1:1, room temperature, five minutes), (3) washed in DI water (4) blown dry in N_2 . After loading into the MO-CVD system, no in-situ cleaning procedure was used, although they were heated to about 1100°C in H_2 before growth was begun.

GaN Growth

As just noted, only R-plane sapphire was available during the early part of this contract period (and also later, when so-called basal plane oriented substrates were found not to be so). Thus MO-CVD growth of GaN was first optimized for growth on R-plane material. Later, re-optimization for growth on basal plane sapphire required only small alterations of the growth parameters, flow rates, and growth temperature.

It became clear immediately that $(\text{CH}_3)_3\text{Ga}$ and NH_3 were forming a low temperature addition compound. A light grey powder dusted the walls of the reactor and single crystals (by X-ray diffraction) could not be grown. Here it was assumed that particles of the solid-phase addition compound fell on the substrate, resulting in very rapid decomposition and very rapid, non-single crystal growth. One possible solution was to replace the $(\text{CH}_3)_3\text{Ga}$ with $(\text{C}_2\text{H}_5)_3\text{Ga}$, which might not form an addition compound. This works in the In-PH_3 system. However, we had no guarantee that this would work here and we would have to wait to receive the $(\text{C}_2\text{H}_5)_3\text{Ga}$ source. Another possible solution would be to reduce the growth pressure to lower the pressures of both the metalorganic species and the NH_3 . This would require complete re-optimization of growth parameters. This was not attempted, because a third and more simple solution was obvious; keep the metalorganic stream separated from the NH_3 until they mixed directly over the surface of the substrate. Thus a tube was connected to the metalorganic inlet at the top of the reactor and the metalorganic stream was discharged through a horizontal nozzle close to the upper surface of the substrate. (The vertical reactor chamber had been designed to do this.) This procedure led immediately to single crystal growth, although use of the R-plane substrates resulted in a non-planar morphology.

This method of avoiding the formation of the addition compound results in non-uniform growth, since one side of the substrate surface is rich in Ga from the metalorganic inlet nozzle and the other side is rich in NH_3 . (See Figure 3).



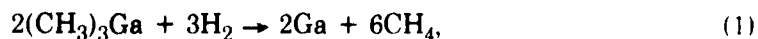
Figure 3. MO-CVD Epilayer AlGaIn No. 42 Growth on Sapphire Substrate. (Mag. 3.75 \times)

If we were to continue this project we would (1) rotate the substrate during growth to attain at least radial symmetry (2) try another metalorganic Ga source or (3) try growth at reduced pressures.

With the flow geometry and gas mixing just described, it quickly became apparent that the temperature of the tip of the Ga nozzle affected the crystal growth significantly. The tip was very close to the hot substrate. The $\text{H}_2/(\text{CH}_3)_3\text{Ga}$ stream flowing through it keeps the tip cool. If the stream were too slow, the tip got hot and the $(\text{CH}_3)_3\text{Ga}$ pyrolyzed inside the tube, coating it with Ga and reducing the Ga fugacity leaving the nozzle. If the stream were too fast, it blew the NH_3 away from the surface of the substrate so that the Ga-NH_3 reaction occurred beyond the substrate. Optimization of the volume flow rate through the inlet tube (tip temperature) and linear flow rate over the substrate surface (NH_3/Ga ratio) led to a 3.5mm ID quartz $(\text{CH}_3)_3\text{Ga}$ nozzle placed 5-20mm to one side of the substrate. This optimized the uniformity of the growing film at the center of the one-inch susceptor.

A resultant problem, associated with this geometry optimization, was the cracking of the substrate during purging before the beginning of a growth run. Here cold H_2 at a high flow rate, impinged on the heated sapphire. To avoid this problem, purging was done in two steps. First, a high flow rate of H_2 impinged on a cold substrate. Then the substrate was heated, but the H_2 flow rate was reduced.

As already noted the growth was non-uniform because of the non-radially symmetric placement of the Ga inlet nozzle (For the purposes of this contract, uniform large area epilayers were not required). Close to the nozzle, the NH_3 pressure was nil. It was "blown away" by the $(\text{CH}_3)_3\text{Ga}/\text{H}_2$ stream and no growth occurred. Next a very Ga rich growth layer appeared. Here, GaN deposited but it was usually not good single crystal material. The material was opaque with both Ga and C precipitation (X-ray dispersive analysis on the SEM). Since H_2 is inherently involved in the decomposition of $(\text{CH}_3)_3\text{Ga}$:



N_2 was substituted for the normal H_2 flow through the $(\text{CH}_3)_3\text{Ga}$ bubbler, but the precipitation was not affected. Beyond this opaque region was a transparent region of uniform single crystal growth. This was the good single crystal region. Its relation to the Ga rich region can be seen in Figure 3. Here the resistivity (10^{-2} to 10^{-1} ohm-cm) was about 10 times higher than in the opaque Ga-rich region. It is anticipated that rotation of the substrate during growth would increase the extent of this uniform region; the Ga-rich regime confined to the periphery of the wafer.

In the early growth runs on R-plane substrates, the optimum substrate temperature was found to be 980°; however, with basal plane substrates an optimum temperature of 850°C was deduced. The flow rates in this case were 1.5l/min of the H_2 - NH_3 mixture, and 1.18l/min of H_2 through the TMG bubbler yielding a TMG concentration in the reactor of 0.014 percent. In both the early R-plane substrate runs and the basal plane runs, the crystal quality was dependent on the NH_3 concentration. Only whiskers of GaN grew when the NH_3 concentration was 8.5 percent but good single crystal growth occurred at a concentration of 75 percent. The flow rate of the H_2 - NH_3 mixture could be adjusted during growth to maximize deposition on the substrate. If the flow rate were too low, the TMG diffused up-stream forming some GaN, but more of the TMG- NH_3 addition product. These materials would coat walls of the reactor above the hot substrate. If the flow rate were too high, much of the GaN was deposited on the susceptor below the substrate and on the hot upper portions of the quartz pedestal.

The optimal conditions deduced for basal plane growth were a substrate temperature of 850°C, an NH_3 flow rate of 3.5 liter/min and a H_2 flow rate of 740 ml/min through the $(CH_3)_3Ga$ bubbler held at 0°C. These flows result in 0.026 percent $(CH_3)_3Ga$ in the reactor.

As already indicated the morphology of the GaN crystals grown on R-plane sapphire was non-planar. These exhibit prism plane facets. It was also observed that the facets became smaller, the surface more planar, as the NH_3 flow rate was increased. As expected, growth on basal plane sapphire was always planar, with frequent indications of step growth (see Figure 4).

X-ray diffraction was used to establish the crystallinity of the grown layers, their orientation, and the orientation of the sapphire substrates. On basal plane sapphire, only single crystal basal plane GaN grows; only sharp (0002) basal plane Bragg reflection is observed. On R-plane sapphire, single crystal prism plane GaN grows (the c-axis is in the plane of the substrate). These results agree with similar observations of halide-hydride VPE grown GaN. If the basal plane sapphire is not exactly on axis only polycrystalline GaN results.

Crystal thickness was measured by two methods. First, the crystals could be cleaved and their cross sections viewed directly by the optical microscope or by SEM (Figure 5). Second, interference fringes in the infrared reflectivity of thin (1-5 micron) uniform layers could be directly correlated to thickness.



Figure 4. AlGaIn No. 42 Showing Step Growth and Hexagonal Symmetry Defect. (SEM 10,000X)



Figure 5. Cleaved Cross Section of AlGaIn No. 45. 4.5 μ m of AlGaIn on 11 μ m of GaN on Basal Sapphire Substrate. (SEM 2,200X)

From these measurements, thicknesses of 2-60 micron and growth rates of 15-20 micron/hr have been deduced.

Hall and resistivity measurements showed that, like all VPE grown GaN, the crystals prepared by MO-CVD were n-type with carrier densities of $1.6 \times 10^{19}/\text{cm}^3$. From electron microprobe analysis we have learned that, unlike the case of some VPE crystals, Si is not a major shallow donor contaminant here (quartz reactor walls are cold). Hence, we conclude that the dominant shallow donor is a native defect, probably a N vacancy. The concentration is 5-10 times greater in MO-CVD than in VPE crystals. Since such material was degenerate and Schottky barriers onto it became ohmic tunneling contacts, it became necessary to compensate the material two to three orders of a magnitude.

Compensation

Our previous studies¹⁵ based on low temperature photoluminescence characterization of intentionally doped GaN grown by halide-hydride VPE, had shown that Be, Mg, Zn, Cd, Ge and Li were all "shallow" acceptors, but deep (200-250 meV) by conventional semiconductor standards and that C was a very deep acceptor. Of these, only Li could be introduced by post-growth diffusion. Only Li has a large enough diffusion constant to form a compensated layer of measurable thickness at 1100°, the maximum temperature at which GaN can be held in an NH_3 ambient to prevent surface decomposition. However, we desired to prepare uniformly doped bulk layers of compensated GaN. Thus, the compensation doping had to be done in-situ, during the crystal growth process itself.

We selected Zn for this purpose for three reasons: (1) it was readily available as a high purity, semiconductor grade metalorganic compound, $(\text{C}_2\text{H}_5)_2\text{Zn}$, (2) there was much experience with zinc as a donor for other semiconductors, and (3) its vapor pressure would be easily controlled by the H_2 flow rates and thermostating baths available.

We began with the Zn source at 20°C, bubbling 2.3 ml/min of H_2 through it. After mixing with the remaining H_2 from the Ga source and with the (740 ml/min) dilutant H_2 , the Zn was introduced through the nozzle at a concentration of 0.005 percent. Fortunately, the growth characteristics and the surface morphology of the GaN grown remained unaffected by the introduction of the Zn. The resistivity increased about a factor of 10, corresponding to a free electron density decrease to about $5 \times 10^{18} \text{ cm}^{-3}$.

¹⁵ L.B. Ta, Ph.D. Thesis, University of Southern California (1981).

This was still one to two orders of magnitude too high for the preparation of good, non-tunneling Schottky barriers. (We predicted that a net carrier concentration of less than 10^{17} cm^{-3} would be necessary). Hence the Zn flow rate was increased. To our surprise no further increase in resistivity was observed. The Zn flow rate was increased drastically. The GaN layers continued to grow with good surface morphology but the resistivity remained fixed. At the highest Zn flow rate, we deduced from electron microprobe analysis that 9.6 percent Zn had been incorporated! By X-ray dispersive analysis (without host absorption corrections) this figure was 6.6 percent (It is noted here, that for these high Zn concentrations, the Zn incorporation rate is no longer linear in Zn flow rate through the reactor) and the resistivity remained constant.

This result was highly unusual. Where was this large amount of Zn, and why was it electrically inactive? We guessed that so much Zn could not be soluble in GaN. Thus, we searched for evidence for a second phase, particularly for Zn_3N_2 , a cubic crystal. No evidence for precipitation was seen either by transmitted light, using an optical microscope, or by SEM observations.

Furthermore, no new lines appeared in the X-ray diffraction patterns. Thus, we concluded that the system was single phase. Next, we examined the diffraction patterns for the influence of Zn on the position and width of the diffraction line. No clear-cut correlations were observed, however. Hence, we note, that on these basal plane epilayers only one major diffraction peak is observed, that corresponding to the unit cell in the uniaxial direction only. Furthermore, the width of this line seems influenced more by where on the epilayer the observation is made, Ga-rich or NH_3 -rich, than by the Zn content presumably because the tetrahedral covalent radius of Zn is only 4 percent larger than that of Ga. We anticipated that Zn incorporated on a Ga site as an acceptor (it does compensate n-type material somewhat, as already remarked) could be close-pairing with a N vacancy to produce an electrically inactive pair. N vacancies would have to be generated, presumably under the influence of a mass-action law, to hold the net electron concentration fixed, or Zn on a Ga site could be pairing with interstitial Zn. The latter should be a donor again leading to electrically inactive pairs.

At this stage, we had several options on how to proceed: (1) try to deduce why Zn becomes electrically inactive and how to overcome this, (2) switch to another acceptor

for doping during growth, for example, Li, (3) use post-growth diffusion of Li to produce a thin compensated layer near the upper surface of the highly conducting N-type GaN layer, or (4) use ion implantation to achieve the same result.

As described below, implantation studies had already been started, and compensation in thin layers by Be implants was beginning to be achieved at this time. Thus, we decided to continue producing partially compensated, Zn doped, planar, basal plane GaN layers as input to this phase of the program, and to expand our research efforts to the AlGa_xN alloy system.

AlGa_xN Alloys

During the last six weeks of this program we attempted to grow the AlGa_xN alloys. These were done without Zn compensation, because of the already noted success of the Be ion implantation work. The MO-CVD system already contained a (CH₃)₃Al bubbler and we anticipated that the Al:Ga ratio incorporated in the solid would be identical to the admitted gas flow ratio.

We started with an Al:Ga molar flow rate ratio of 1:5, using the same optimized flow and temperature conditions previously deduced for GaN on basal plane sapphire. However, the layers grown were not single crystal. It was necessary to increase the substrate temperature from 850° to 1000°, while holding all the flow parameters constant, in order to achieve single crystal growth. Under these conditions, good single crystals (x-ray diffraction) with planar morphology (SEM) were grown on basal plane sapphire substrates (Figure 6) or on pure GaN (Figure 5) previously grown on basal plane sapphire (one run only), and as much as 73 mole percent Al could be incorporated. Samples were immediately made available for implantation compensation, and the materials characterization was minimal, since the contract was drawing to a close.

However, it was noted that the resistivities of these crystals corresponded to a free electron density of 10^{19} - 10^{20} cm⁻³, about a decade higher than that for pure GaN. In addition, electron microprobe analysis indicated that Si at about 10^{20} /cm³ was the dominant impurity. From our previous work with GaN, we knew that Si was a shallow donor (25 meV) and a common contaminant in GaN, particularly in GaN grown in systems built from fused quartz. Thus, our attention was immediately directed to the metalorganic quartz inlet nozzle close to the substrate. During AlGa_xN growth, a film formed on the surface of the nozzle. This was not observed for the growth of pure GaN.



Figure 6. Planar Surface of GaN No. 23 on Basal Plane Sapphire. (SEM 20,000X)

However, the substrate temperature for AlGa_N growth was 1000°, not 850° used for Ga_N. Hence at 1000° the quartz inlet tip gets hotter by convection, conduction and/or radiation, and the metalorganic molecules pyrolyze on the surface, depositing both Ga and Al. Al is very reactive with SiO₂ at 1000°, releasing SiO into the reactant stream. It was this species which presumably doped the growing crystals. The solution to this problem was obvious; use a high density alumina tube as the inlet nozzle instead of fused silica. However, the contract period expired before this solution could be implemented. In spite of this, and in spite of the high Si donor content of the available crystals, ion implantation was successful, as described below, in compensating the AlGa_N alloys for the fabrication of UV sensitive Schottky barriers.

Optimized Growth Procedure

The following procedure was developed for growing epitaxial layers of GaN and AlGaN on sapphire substrates by MO-CVD.

A. SUBSTRATE PREPARATION

The polished sapphire substrates were cut to size and then cleaned in:

1. Benzene
2. Trichlorethylene
3. Methanol or Isopropyl Alcohol
4. Deionized water

Dry with N_2 gas.

Before growth the substrate was etched as follows:

1. 15 min in hot H_3PO_4 - H_2SO_4 1:1 mixture.
2. Rinse with DI water and dry with N_2 gas.

B. PREPARATION BEFORE THE GROWTH RUN

1. Fill TMG dewar with ice water so that equilibrium $0^\circ C$ TMG vapor pressure can be reached.
2. Open cooling water for RF generator.
3. Pump down the system until the pressure in the system is lower than 25μ . Turn off the pump.

C. FLUSHING THE SYSTEM

1. Flush the system with nitrogen.

D. INCREASING TEMPERATURE

1. Turn on the RF generator.
2. Heat up graphite susceptor slowly.
3. At a temperature of $400^\circ C$, switch system N_2 to H_2 .

4. Keep increasing the susceptor temperature to 1100°C to do thermal etching.
5. Start the NH_3 flowing through the system.
6. Wait for five minutes, then reduce temperature to growth temperature.

E. AT GROWTH TEMPERATURE

1. Close by-pass valve of TMG and open its inlet and outlet valve at the same time.
2. Adjust all the flow rates to growth conditions.
3. After observing GaN deposition (a few minutes), open TMA for AlGaIn growth and DEZ for compensation.
4. Grow for about two hours, then shut off the system.
The typical growth rate is 15-20 $\mu\text{m}/\text{hour}$.

F. SHUT OFF THE SYSTEM

1. Shut off TMG and TMA or DEZ.
2. Continue flowing NH_3 (and H_2) to avoid surface decomposition.
3. Lower the temperature slowly.
4. At $T \leq 400^\circ\text{C}$, shut off NH_3 flow.
5. At $T \leq 200^\circ\text{C}$, change H_2 flow to N_2 .
6. Open the by-pass valve in metalorganic source bubblers to flush out all the residual deposits in the by-pass lines.
7. Finally, shut off all flow meters and cylinders, close exhaust valve and pump down.

G. LOADING AND UNLOADING THE SAMPLE

1. Before opening the system to air, back-fill the reactor with N_2 .

Discussion of Materials Preparation and Characterization

The objectives of the materials preparation aspects of this contract, the attainment of suitably doped, planar, single crystal epilayers of both GaN and of AlGa_N on which UV sensitive, Schottky barrier photovoltaic junctions could be prepared, was clearly realized. In the time allotted, 54 samples were grown. These are tabulated in Table 1 with growth parameters and results. We have demonstrated that the MO-CVD technique can be used to prepare planar larger area single crystals of GaN and AlGa_N.

To avoid the formation of the solid-phase low-temperature metalorganic — NH₃ addition compound, we used a metalorganic inlet tube close to one edge of the substrate. This resulted in non-uniform growth. For uniform large area growth, this condition could be improved by rotating the substrate during growth. In our MO-CVD system, this would simply involve installation of a rotary vacuum seal and motor drive for the substrate supporting pedestal. But, perhaps, better yet, the formation of the addition compound might be avoided by either using (C₂H₅)₃Ga instead of (CH₃)₃Ga as the source, or by operating at reduced (< 1 atm) reactor pressure. Both of these methods work in the In-P system. Our MO-CVD system was designed to allow both alternatives easily. Thus, there remain several options open for achieving large area uniform growth.

The GaN crystals grown were always of a resistivity too low to permit the fabrication of non-shortening Schottky barriers. (Ion implantation of an acceptor, Be, was used eventually to overcome this problem). Only Zn was used during growth to compensate the material, but only one decade of compensation out of the three required could be achieved. Remarkably, up to 9% Zn was introduced into the crystals, yet the net electron density remained in the 10¹⁸cm⁻³ range, and the crystals remained single phase. A more comprehensive study of this phenomenon by Hall measurements, low temperature photoluminescence, C-V, x-ray lattice diffraction and chemical analysis, especially associated with annealing and Ga/NH₃ variations during growth might resolve the question of how this large amount of Zn is being incorporated, and may suggest methods

TABLE 1. SUMMARY OF MO-CVD GROWTH RUNS

Sample No.	Substrate Orientation (1)	Growth Temperature (°C)	MO H ₂ (2) (cc/min)	NH ₃ H ₂ (4) (cc/min)	NH ₃ (cc/min)	TMG H ₂ (5) (cc/min)	DEZ H ₂ (6) (cc/min)	TMA H ₂ (7) (cc/min)	Room Temp. (°C) (8)	TMG Vapor Pressure (Torr)	DEZ Vapor Pressure (torr)	TMA Vapor Pressure (torr)	Single Crystal	Resistivity (10 ⁻³ Ω-cm)	Thickness (μm)	Mobility (cm ² /V-sec)	Composition
1	R	990	967	266	111	5				65			No				
2	R	757	967	266	131	4				65			No				
3	R	897	1463	760	131	4				65			No				
4	R	900	1463	714	131	2				65			Yes				
5	R	1012	246	1463	131	3				65			No				
6	R	990	2204	2204	85	3				65			Yes				
7	R	985	927	1923	131	3				65			Yes				
8	R	1000	243	1923	131	3				65			Yes				
9	R	980	547	1390	131	2				65			Yes				
10	R	980	927	1390	131	2				65			No				
11	B	975	547	1390	72	2				65			NO				
12	B	960	547	1390	131	2				65			Yes				
13	B	910	927	1390	131	2				65			Yes				
14	R	980	927	1390	131	2				65			No				
15	R	980	1216	1390	131	2				65			Yes				
16	R	975	1178	1390	131	2				65			Yes				
17	B	985	722	370	1123	2				65			No		7		
18	R	975	722	570	2547	2				65			Yes				
19	R	975	722	570	2547	2	3		21	65	12		Yes	20	3	3	
20	B	950	380	570	3004	2	3		21	65	12		Yes				
21	B	950	760	570	2808	2	2		21	65	12		Yes				
22	B	450	760	570	3853	2	2		21	65	12		Yes				
23	B	945	760	570	3853	2	2		21	65	12		Yes	0.27	3	61	
24	B	828	760	570	3853	2	2		20	65	12		Yes				
25	B	855	760	570	3853	2	2		21	65	12		Yes	1.5-754			
26	B	850	760	570	3853	2	2		21	65	12		Yes	1.5-48			(9)
27	B	815	760	570	3853	2	2		23	65	13		Yes	4-44		3.9	(10)
28	B	815	760	1520	3853	2				65				45			

TABLE 1. SUMMARY OF MO-CVD GROWTH RUNS (CONCLUDED)

Sample No.	Substrate Orientation (1)	Growth Temperature (°C)	MO H ₂ (2) (cc/min)	NH ₃ H ₂ (4) (cc/min)	NH ₃ (cc/min)	TMG H ₂ (5) (cc/min)	DEZ H ₂ (6) (cc/min)	TMA H ₂ (7) (cc/min)	Room Temp. (8) (°C)	TMG Vapor Pressure (torr)	DEZ Vapor Pressure (torr)	TMA Vapor Pressure (torr)	Single Crystal	Resistivity (10 ⁻³ Ω-cm)	Thickness (μm)	Mobility (cm ² /V-sec)	Composition
29	B	800	760	1520	3853	2	7		23	65	13			34-102			(11)
30	B	850	760	1520	3853	2	6		25	65	15			34-77		13	(12)
31	B	850	760	1520	3853	2	6		23	65	13						
32	B	850	760	1520	3853	2				65							
33	B	850	760	1520	3853	2				65							
34	B	850	760	1520	3853	2				65				0.13	12	35	
35	B	850	760	1520	3853	2				65				1.7	14	47	
36	B	850	760	1520	3853	1				65			Yes				
37	B	850	760	1520	3853	2				65			No				
38	B	850	760	1520	3853	2				65							
39	B	850	760	1520	3853	2				65							
40	B	850	760	1520	4225	1				65			Yes	2.3	66		
41	B	850	760	1520	3853	2		3	25	65		6	No	6.8	20		(13)
42	B	950	760	1520	3853	2		3	22	65		5	No	6-45	8	67	(14)
43	B	1000	760	1520	4615	2		3	22	65		5	Yes	14-8	7	304	(15)
44	B	900	760	1520	4225	2		3	22	65		5	No	0.9	8		(16)
45	B	1000	760	1520	4615	2		4	27	65		5	No	14-41	5		(17)
46	B	1000	(3) 760	(3) 800	4225	1(3)		3(3)	21	65		5	No	31-155			
47	B	1000	(3) 200	(3) 400	4225	1		(3) 1	21	65		5	No	3-19			
48	B	1000	760	1520	5000	2		3	20	65		4	No	11-134			
49	B	1000	760	1520	4225	2		3	21	65		5	No	2-7			
50	B	1000	760	1520	4225	2		3	21	65		5	No				
51	B	1000	760	1520	4225	2		3	20	65		4	No				
52	B	1000	760	1520	4225	2		3	21	65		5	No				
53	B	1000	760	1520	4225	2		3	21	65		5	No				
54	B	1000	760	1520	4225	2		3	29	65		8	Yes	18-820			

FOOTNOTES TO TABLE 1

1. R R-plane sapphire.
B Basal plane sapphire.
2. H_2 flow rate mixed with H_2 through MO bubbler and injected through inlet nozzle in reactor.
3. N_2 used instead of H_2 .
4. H_2 flow rate mixed with NH_3 .
5. H_2 flow rate through TMG $((CH_3)_3Ga)$ bubbler.
6. H_2 flow rate through DEZ $((C_2H_5)_2Zn)$ bubbler.
7. H_2 flow rate through TMA $((CH_3)_3Al)$ bubbler.
8. Room Temperature: DEZ and TMA bubbles are kept at room temperature; TMG bubbler is held at $0^\circ C$.

Composition by electron microprobe analysis
(Zn:wt. %, X in $Al_xGa_{1-x}N$, mole %)

9. Zn 0.39-0.46%
10. Zn 0.29-0.45%
11. Zn 2.8-7.0%
12. Zn 1.5-9.5%
13. X 34.5-73.1%
14. X 11.9-22.5%
15. X 4.2-6.8%
16. X 8.1-19.8%
17. X 36.3-39.3%

for keeping the Zn active as an acceptor, so that higher levels of compensation could be achieved.

Instead of Zn, other acceptors should be tried. In particular, the acceptor Li can be introduced easily by diffusion (it is the only impurity that can be easily diffused into GaN) and it is readily available as a metalorganic compound, for use in the MO-CVD growth system. Thus, there are possible options for obtaining appropriately compensated bulk material other than by ion implantation as used here.

The AlGa_N crystals prepared during this contract must also be considered to be first-order approximations. The epilayers were single and planar, but in addition to lack of spatial thickness uniformity control, as with pure GaN control of the Al:Ga ratio, and hence the wavelength sensitivity of the final devices was not demonstrated. If the growth rate is made uniform, as discussed above, then there is no simple reason why the Al:Ga ratio in the grown crystal should not depend simply on the preset Al:Ga metalorganic flow rate. Hence, we anticipate that this will not be a major problem.

Compensation of the AlGa_N crystals was achieved by ion implementation of Be. However, we have demonstrated that in these crystals, as opposed to the pure GaN layers, the high electron density was due to Si impurities deriving from a hot fused silica inlet nozzle. Replacement of this nozzle with an alumina tip should obviate this problem. Then it is not clear whether or not the native nitrogen vacancy donor will dominate the electrical characteristics, nor how it will depend upon the Al:Ga ratio. This will determine how much compensation (as described above) will be necessary to achieve suitable material for Schottky barrier fabrication.

Thus, although the GaN and AlGa_N material preparation and characterization results reported here have clearly demonstrated device feasibility, the attainment of a viable materials technology must involve a more thorough assessment of the preparation techniques, particularly with regard to growth uniformity, compensation and composition control in the alloy system.

ELECTRICAL EVALUATION

Epilayer Samples

A typical AlGaIn epilayer grown by MO-CVD on an irregularly shaped piece of sapphire with dimensions of approximately 10 mm by 20 mm is shown in Figure 3. Near one edge of the sapphire was a very dark region about 5 mm in diameter where the stream from the metalorganic nozzle impinged. The dark coloration was caused by gallium inclusions in the epilayer. Extending away from the black area the deposit became lighter in color, having a whitish or yellowish powdery appearance. Then the powdery material thinned out, and the surface took on a pearly appearance, showing interference colors. Five to ten millimeters away from the black spot, the epitaxial layer ended. The pearly ring was the only area in which good Schottky diodes were produced, because the highest quality crystal occurred in this region.

The small size of the sample and the variation in quality made it difficult to characterize the material. Cutting samples for Hall measurements was also difficult. Sawing the sample was time consuming and sapphire did not always break where scratched by a diamond scribe.

In preparation for the fabrication of Hall test chips, samples were cleaned successively in chloroform, acetone and nitric acid and rinsed in DI water. A Hall sample was cleaved off after scribing the sapphire side of the sample with a diamond stylus. Contacts were made to the corners of the sample by soldering lengths of No. 40 tinned copper wire with pure indium.

Figure 7 is a Nomarski photograph of a cleaved AlGaIn epilayer on a sapphire substrate. This type of photo provided thickness data required for Hall calculations.

Transport Properties

Carrier concentration and mobility are measured routinely on the computerized material test station at Honeywell Corporate Technology Center, shown in Figure 8. The van der Pauw samples are mounted in a test fixture which is inserted between the poles of the Hall magnet. Normally, Hall measurements are made at two temperatures, 300°K and 77°K, to obtain information on the density of shallow donors by the "freezeout" that occurs during this temperature change. However, all measurements of carrier concentra-



Figure 7. Cross Section of Cleaved Sample GaN35. Thickness of GaN Layer, 14 microns. Magnification, 492 \times . Substrate is sapphire.

tion in AlGaIn resulted in large values of n , approximately 10^{19} electrons cm^{-3} and the difference between measurements at room temperature and those at liquid nitrogen temperature were small. The distribution of electrons at these high concentrations is degenerate so that transport measurements as a function of temperature provided little information about the donors responsible for the high carrier concentration.

Another Hall system is available in which the sample can be controlled at any temperature between 4.2K and 400°K. This system was used for the wide temperature range Hall measurements discussed in Section 5.

Ion Implantation

Acceptor atoms may be introduced by ion implantation for the purpose of compensating the high donor population. The concentration of implanted ions as a function of depth may be accurately calculated from the parameters of the target and implanted ions using the theory of Lindhard, Scharff and Schmidt (LSS theory). At a given energy, implanted ions assume a Gaussian concentration profile. A computer program is available for designing a sequence of implantations having energies and intensities that will produce a profile that is approximately flat.

A portion of the epilayer was shielded from the ion beam during implantation to provide an area for the ohmic contact and also to provide material as a control for comparison purposes.



Figure 8. Honeywell's Computerized Materials Evaluation Facility. Hall magnet is at far right. Next to it is the computer console and input and output devices. Rack in center contains computer controlled power supplies and measuring instruments.

Ion implantation always damages the crystal structure, therefore annealing of the sample was necessary. The annealing temperature and duration were dependent on the implanted ion, the target material and the target temperature during implantation. Many of the III-V compound semiconductors are subject to decomposition at annealing temperatures; therefore, steps must be taken to suppress this decomposition. A temperature of 1000°C for one hour has been shown to be adequate to anneal GaN¹⁵ but under these conditions GaN loses nitrogen. However, if the annealing atmosphere is flowing ammonia, nitrogen loss is suppressed.

Ion implantation produced a slight darkening of the surface of the target, possibly due to the formation of F centers. The original color was restored after annealing.

Ion implantation increased the resistivity by carrier compensation. Since the penetration is only a micron or so, the actual carrier concentration values of the implant cannot be determined by Hall measurements or the 4-point probe. It can however, be determined by C-V measurements.

Optical Measurements

In the course of this investigation, two different methods were used for optical measurements. The first system provided a measure of the spectral response of the UV Schottky detector by connecting the device to the high impedance input of a PAR 116 preamp and plotting "open circuit" voltage versus optical wavelength.

For the second technique, the detector output was connected to the input of a Keithley 610B electrometer which was operated in its current sensitive mode. The electrometer produces a virtual short across its input terminal providing a measure of the detector "short circuit" current. This method was used to determine the quantum efficiency of the detectors.

A schematic of the optical test system is shown in Figure 9. The light source is an Oriel Optics quartz high pressure Xenon lamp. The radiation from this lamp is dispersed by a Perkin Elmer quartz prism monochromator fitted with a microprocessor controlled wavelength drive motor. The AlGaIn sample is mounted at the exit slit and its signal can be monitored either on a Tektronix Model 5301 oscilloscope for dynamic measurements, a Keithly 610B electrometer for short circuit current measurements or fed to a PAR lock-in amplifier for recording an open circuit voltage versus wavelength on a Hewlett-Packard XYT recorder. In the last mode, the light is chopped by an EG & G Model 125A chopper which also provides a sync signal for the lock-in amplifier. The measurement of open circuit voltage is the more sensitive of the two due to the noise reduction of the

¹⁵ L.B. Ta, Ph.D. Thesis, University of Southern California (1991).

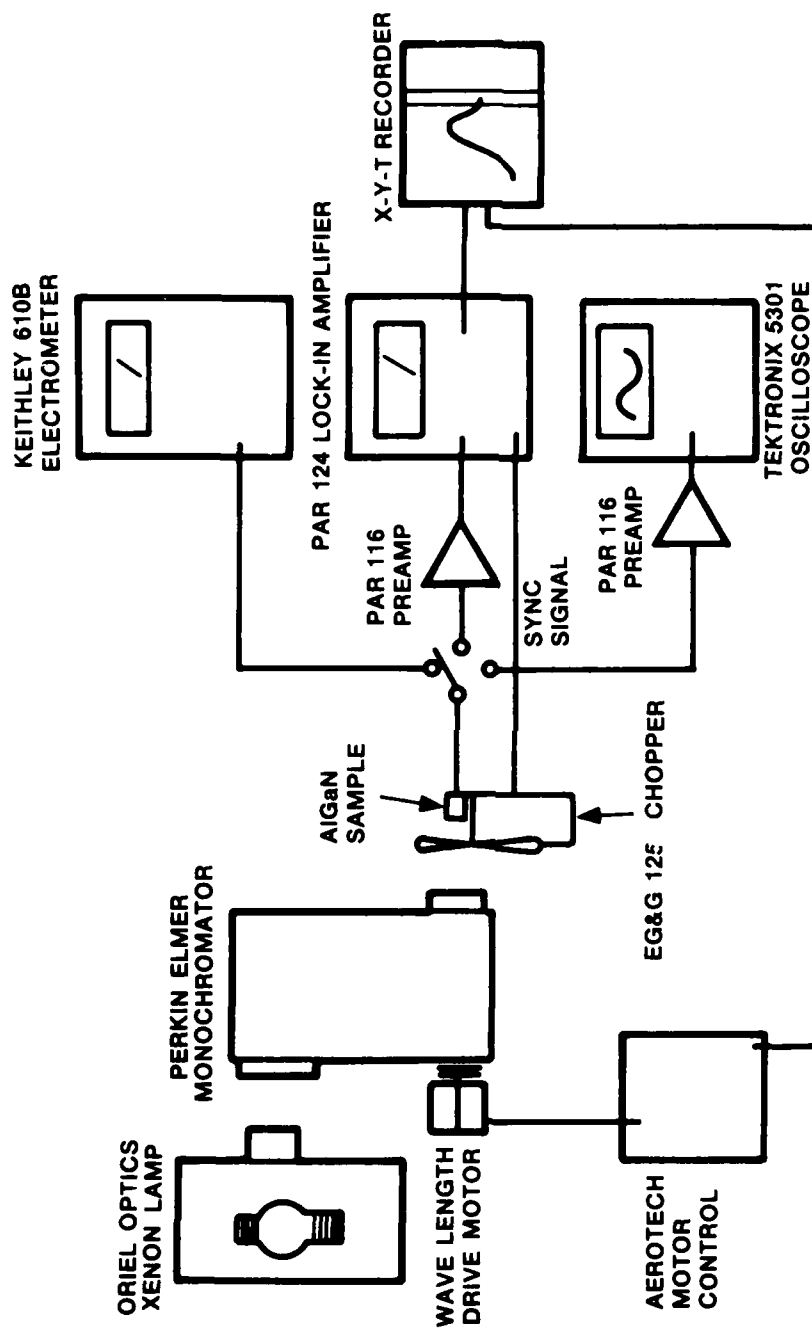


Figure 9. Instrumentation for Optical Measurements

phase-locked technique. The short-circuit current, however, was necessary to determine the detector efficiency. As discussed in the next section, it was not feasible to measure the efficiency of all samples due to lack of sensitivity.

Section 5

Device Evaluation

HALL MEASUREMENTS

The first electrical measurement made on GaN and AlGa_N epilayers at Corporate Technology Center is the Hall measurement. Table 2 is a compilation of results of these measurements. A few observations can be made:

1. Most resistivities are in the 10^{-2} to 10^{-4} ohm cm range.
2. Most mobilities are between 30 and 75 cm^2/Vs .
3. Carrier concentrations are in the 10^{19} cm^{-3} range or greater.
4. Only small changes of resistivity occur between 77°K and 300°K.

A plot of results of Hall measurements versus temperature over the temperature range from 77°K to 400°K is shown in Figure 10. The small variations of the data with temperature are due to electron degeneracy caused by the high carrier concentration. Therefore, it is impossible to use the "freeze out" of shallow states to deduce the nature of the contaminants responsible for the low resistivity.

CONTACTS

Ohmic Contacts —Very little was known about making ohmic contacts to GaN and AlGa_N. L. Anne¹⁶ reported the use of indium as a contact material on GaN. Tin, which has a higher melting point than indium, was another material that we wished to explore. Several dots of pure indium and tin were melted onto epilayers of GaN and AlGa_N. The contact metals easily wet the semiconductor surface.

¹⁶ L. Anne, Ph.D. Thesis, University of Southern California (1979).

TABLE 2. GaN AND AlGaN TRANSPORT PROPERTIES

Sample No.	Thickness microns	77°K				300°K				Remarks
		μ cm ² /Vs	n cm ⁻³	ρ ohm cm	μ cm ² /Vs	n cm ⁻³	ρ ohm cm			
GaNDW 805a	65	40.6	1.2x10 ¹⁹	0.013	63.6	9.2x10 ¹⁸	0.0107	CVD GaN	μ and n from 77° to 400°K	
GaNDW 805b	65	39.6	1.2x10 ¹⁹	0.013	60.5	9.3x10 ¹⁸	0.0107	MO-CVD Zn doped GaN R Plane		
GaN #19	3	3.0	2.9x10 ¹⁹	.02	6.2	1.4x10 ¹⁹	.07	MO-CVD Zn doped GaN Basal Plane		
GaN #23	3.3	60.7	3.7x10 ²⁰	2.7x10 ⁻⁴	50.6	4.1x10 ²⁰	3x10 ⁻⁴	MO-CVD GaN		
GaN #34	11.4	35	1.3x10 ²¹	1.3x10 ⁻⁴	30	1.5x10 ²¹	1.4x10 ⁻⁴	MO-CVD GaN		
GaN #35	14	47.1	7.9x10 ¹⁹	1.7x10 ⁻³	46.7	8x10 ¹⁹	1.7x10 ⁻³	MO-CVD		
AlGaN #42	8.1	67	9x10 ¹⁸	0.01	75	8.8x10 ¹⁹	9.4x10 ⁻³	Al(0.112→224)Ga(0.888→0.776)N		
AlGaN #43	7.1	303.5	5.3x10 ¹⁸	0.0027	180	9.9x10 ¹⁸	2.5x10 ⁻³	Al(0.042→0.068)Ga(0.958→0.932)N		

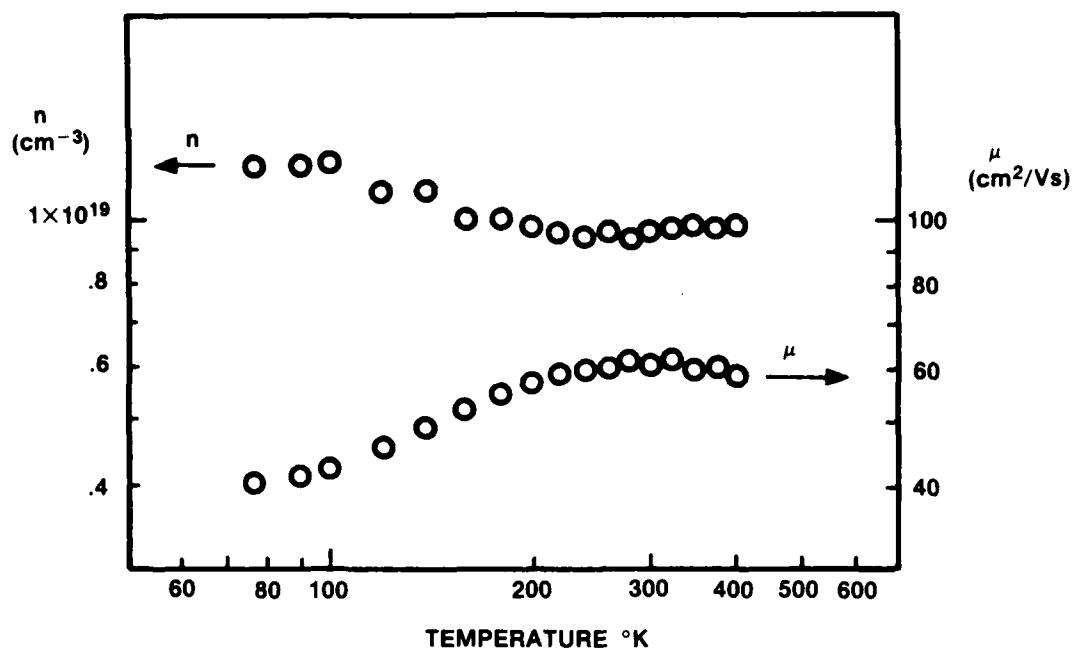


Figure 10. Carrier Concentration, and Mobility as a Function of Temperature for GaN Epilayer.

When probed using the curve tracer, the indium contacts gave linear I-V curves for both GaN and AlGaIn, indicating the suitability as an ohmic contact material. Tin contacts produced linear I-V curves on GaN but nonlinear curves on AlGaIn, (see Figure 11) so it was no longer used as a contact material.

Schottky Contacts —Schottky contacts were made by vacuum evaporating gold through a shadow mask consisting of an array of either 0.75 or 1 millimeter holes onto the semiconductor layer (Figure 12). Gold was selected because it is stable against oxidation, has a high work function, and is easily evaporated to form semi-transparent, conducting electrodes. Initially, the gold dots were 1000\AA thick to provide a durable contact for I-V studies. Gold in this thickness is not transparent, so it was later reduced to 150\AA for optical measurements. The gold contacts on nonimplanted samples gave linear IV traces indicating no rectification was taking place. Satisfactory gold diodes could be formed on ion implanted GaN and AlGaIn. This will be discussed later.



(a) AlGaIn43 (Indium to Indium)



(b) AlGaIn43 (Tin to Tin)

Figure 11. I-V Curves of Ohmic Contacts on AlGaIn No. 43, Indium to Indium (a) and Tin to Tin (b). Vertical 1 ma per div. Horizontal .5V per div.

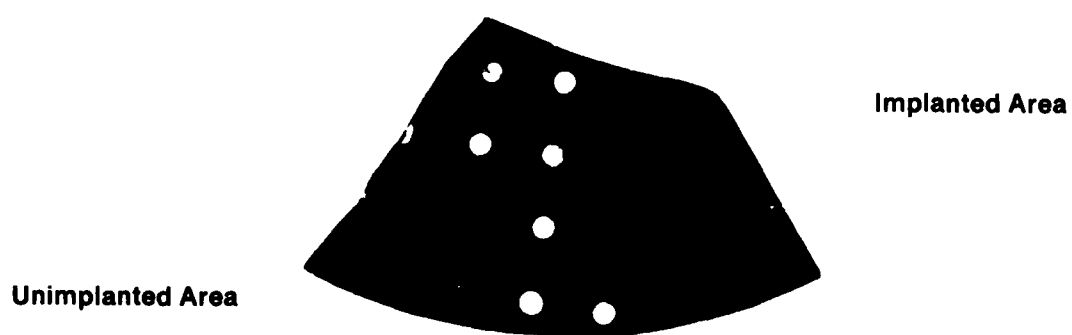


Figure 12. Gold Schottky contacts 1mm in Diameter on Sample GaN 35. Sample had been implanted with Be in upper area. (Mag = 3.75X)

MIS Structure

The lack of rectification in the Schottky contacts was caused by the narrow depletion region through which large tunnelling currents flowed. This is a consequence of the high donor concentration measured to be approximately 10^{19} cm^{-3} . In order to reduce the flow of tunnelling electrons, an MIS structure was created by sputtering a thin (100\AA -- 150\AA) film of Si_3N_4 onto the GaN before metallization. Diodes constructed in this way exhibited only weak rectifying behavior and were not considered useful.

Test Device

Figure 13 shows a test device used for GaN and AlGaIn diode evaluation. A sample with two Schottky barriers and two ohmic contacts is cemented to the base of a TO-5 header. Connection with the feed-through conductor is made with No. 40 tinned copper wire, soldered with indium to the ohmic contact, and with silver paste to the Schottky metallization.

In the future, similar structures can be fabricated from wafers on which multiple layers of different x -values have been grown. In this way, detectors with different spectral responses can be integrated on the same substrate.

Ion Implantation

As mentioned earlier, a high donor concentration in a semiconductor can be reduced near the surface by implantation of acceptor ions. Therefore, we implanted layers of GaN and AlGaIn with beryllium, a convenient acceptor. A multiple step implantation was done on each sample using three different energies and doses calculated by LSS theory to achieve an approximately flat density profile to a depth of 1 micron. The predicted implant density is shown in Figure 14. The following implantation program was employed:

Be ions		
Step No.	Energy (KeV)	Dose ($\times 10^{14} \text{ cm}^{-2}$)
1	40	2.3
2	180	4.6
3	400	6.6



Figure 13. AlGaIn Test Device Showing Two Ohmic Contacts and Two Schottky Barrier Contacts

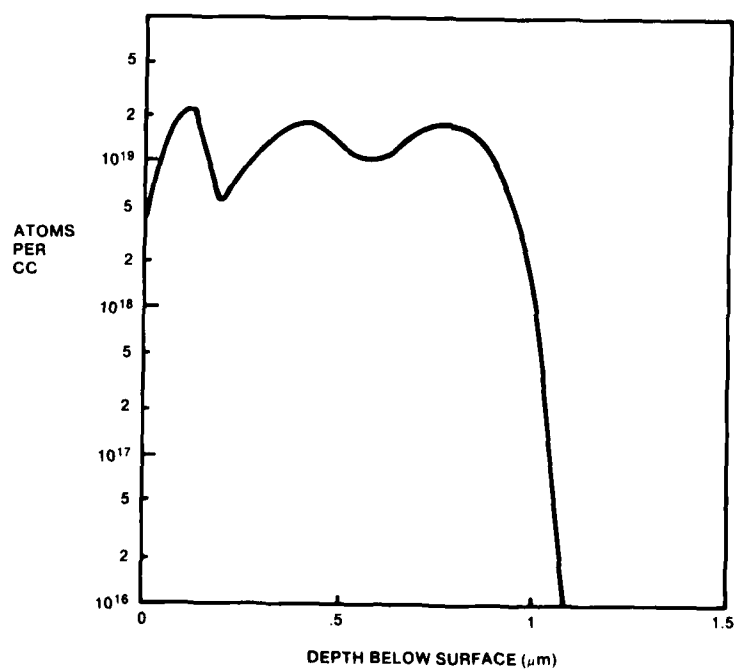


Figure 14. Implanted Beryllium Density Profile, Calculated from LSS Theory

Such a program would produce an average beryllium concentration of $1.35 \times 10^{19} \text{ cm}^{-3}$ to a depth of 1 micron. Parts of each sample were shielded from the ion beam during implantation for later attachment of an ohmic contact and for control purposes. After implantation, the samples were annealed for one hour at 1000°C in flowing ammonia. An array of gold Schottky contacts was vacuum evaporated on the epilayer, (Figure 12) and an indium ohmic contact was melted onto the unimplanted area.

I-V curves were made of the Schottky contacts on the unimplanted and implanted areas. Those formed on the unimplanted GaN and AlGaN were almost linear while those on the implanted area showed the well defined rectifying behavior of a Schottky barrier for both GaN and AlGaN. (See Figure 15) C-V measurements showed a carrier concentration in the implanted layer of 10^{17} cm^{-3} , a reduction by a factor of 100 from the initial concentration. thus it was demonstrated that Schottky barriers can be formed on high carrier concentration GaN and AlGaN after acceptor ion implantation. We were able to operate these photodiodes in the photovoltaic mode for both open circuit voltage and short circuit current measurements. However, attempts to reverse bias the diodes often resulted in their breaking down.

Optical Measurements

The first indication of photoresponse was obtained on the Au/Si₃N₄/GaN MIS diodes previously described. The diodes were reverse biased and illuminated by chopped xenon light. Using a lock-in amplifier and the full intensity of the arc lamp a 1 microampere photoresponse was measured in a high leakage current background. It was not possible to make a spectral response curve, but through the use of interference filters it was determined that the long wavelength cutoff was between 320 and 350 nm, which brackets the wavelength equivalent of the bandgap of GaN.

Photodiode Response Time — The transient response time of the Schottky photodiodes was determined by exposing the devices to chopped xenon radiation and displaying the signal on an oscilloscope after amplification by a PAR No. 114 signal conditioning amplifier. Figure 16 shows the response time to be less than 500 microseconds. The displayed rise time is limited by chopper and amplifier characteristics.

Spectrometric Response — Response curves of implanted AlGaN photodiodes to the xenon lamp source were obtained by measuring the open circuit voltage as a function of wavelength. The resulting curves for detectors from three different wafers are shown in Figures 17, 18 and 19 followed by a tabulation of the data from these curves.

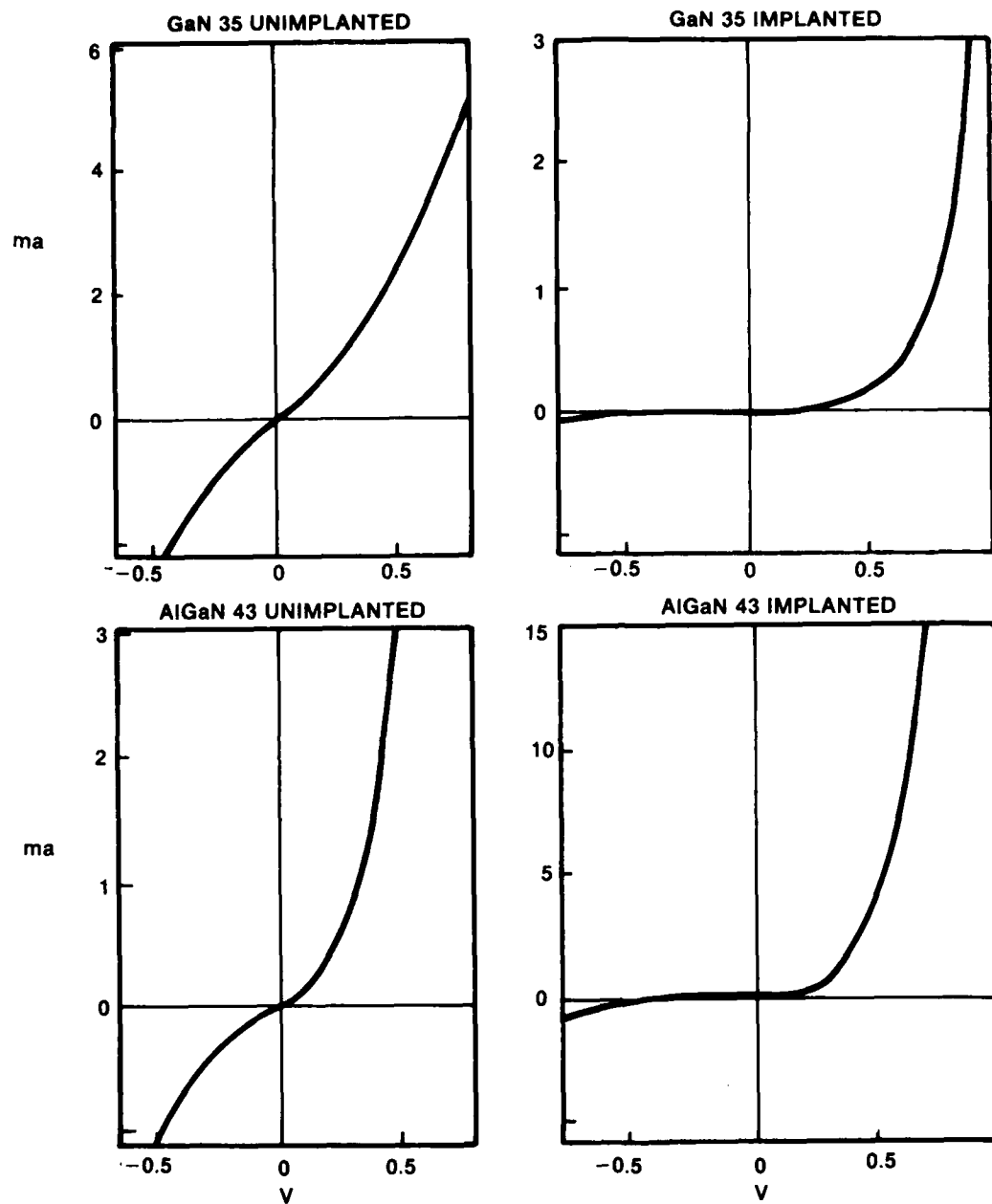


Figure 15. I-V Curves of GaN and AlGaIn, Unimplanted and Implanted with Be

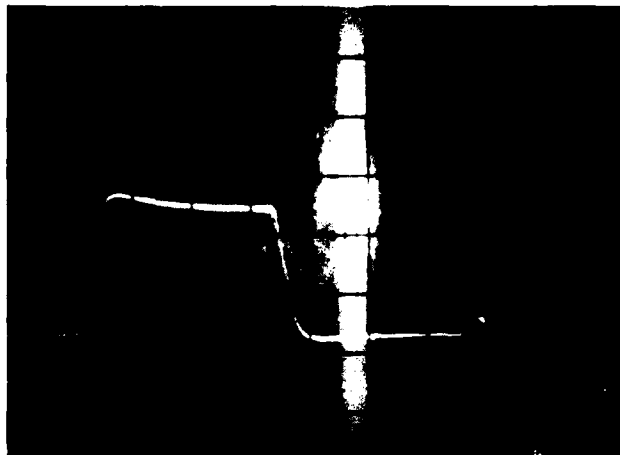


Figure 16. Transient Response of AlGaIn 43. Vertical: Arbitrary Units. Horizontal: 1 ms/div.

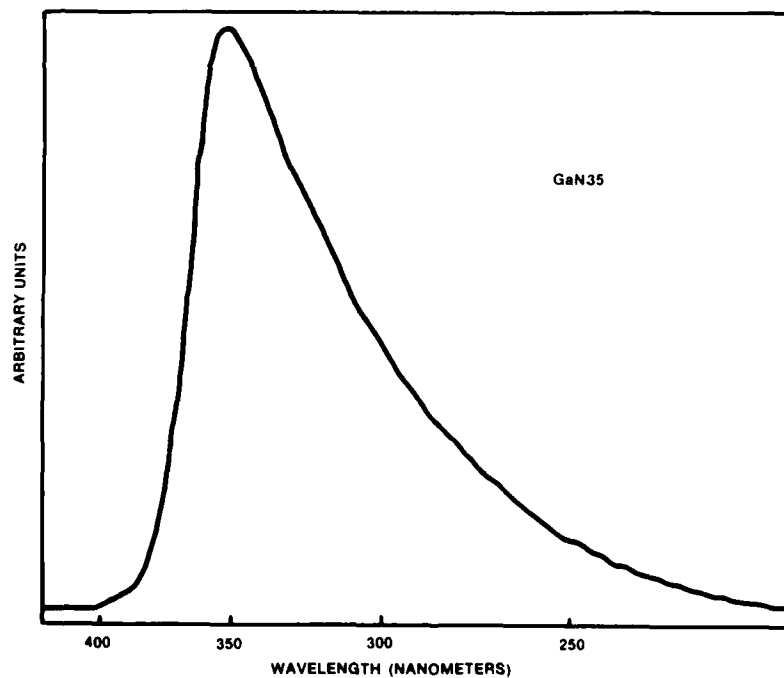


Figure 17. Spectral Response Curve of Implanted GaN Epilayer

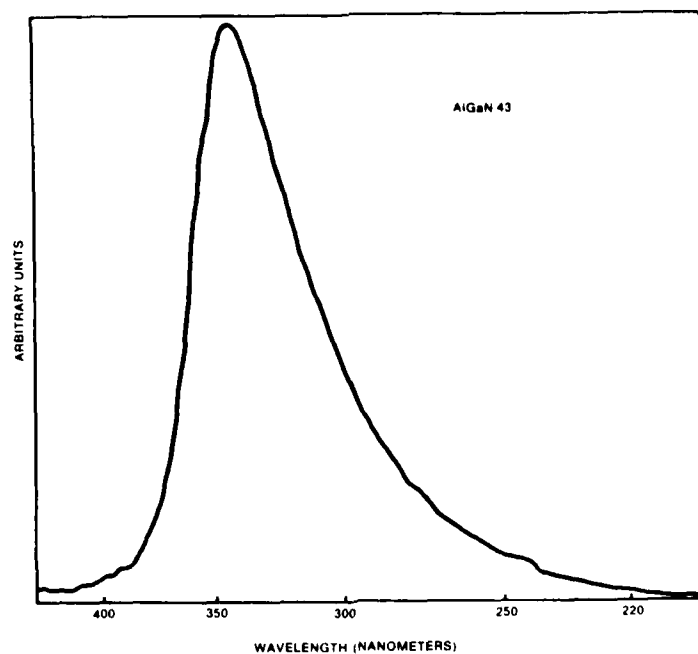


Figure 18. Spectral Response Curve of Implanted AlGaIn Epilayer (AlGaIn 43, $x = 0.042 \rightarrow 0.068$)

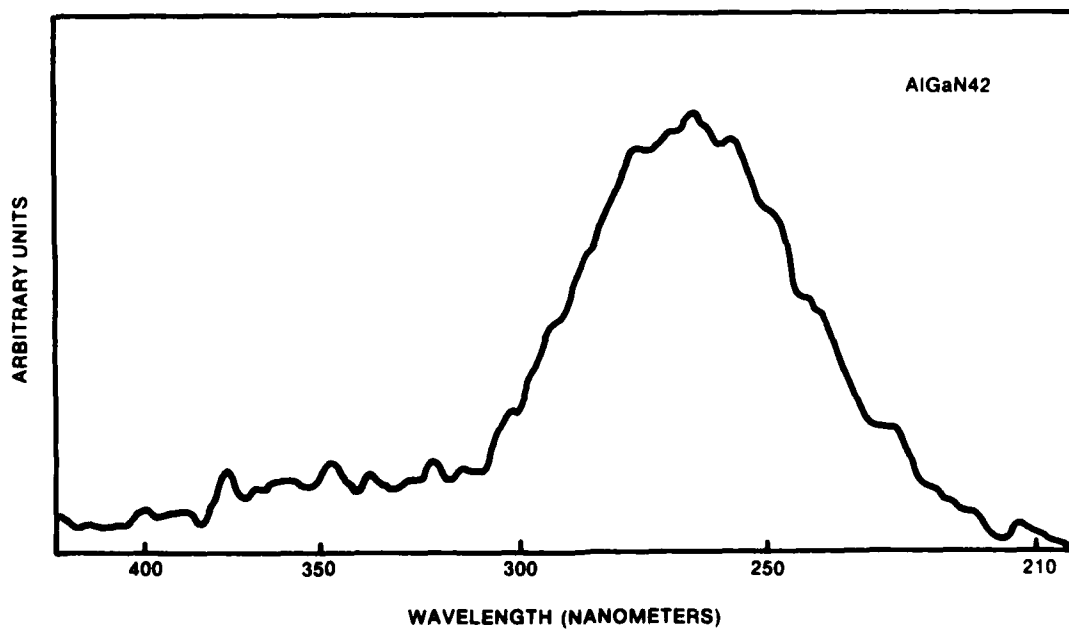


Figure 19. Spectral Response Curve of Implanted AlGaIn Epilayer (AlGaIn42, $x = 0.112 \rightarrow 0.224$, not single crystal).

Spectral Peak

Sample No.	x-value range	(nm)	(eV)	Peak Voltage (μ V)
GaN 35	0	351	3.53	12.7
AlGaN 43	0.04→0.07	343	3.61	14.5
AlGaN 42	0.12→0.22	267	4.64	2.03

It should be noted that samples AlGaN 43 and AlGaN 42 had 0.75 mm diameter contacts while GaN 35 had 1.0 mm diameter contacts. Therefore, although the two detectors produced approximately the same open circuit voltage, AlGaN 43 required less optical power. In addition, AlGaN 42 was not single crystal, which would account in part for its markedly lower sensitivity.

The measurement of open circuit voltage proved extremely useful in the determination of the shape of the spectral response of the UV detectors. It was especially valuable in the measurement of the extremely small signals from AlGaN 42, which as mentioned was not single crystal. However, open circuit voltage cannot be used to determine quantum efficiency. This determination requires the measurement of short circuit current. The external quantum efficiency η of a detector at frequency ν is defined as

$$\eta = \frac{I_D/q}{P/h\nu} \quad (2)$$

where h is Planck's constant, q is electronic charge, and I_D is the current out of the detector resulting from the incident optical power P . It is, therefore, a ratio of the number of electrons/sec. leaving the detector to the number of photons/sec. striking the detector.

The measurement of quantum efficiency in this investigation used short circuit current for I_D . It is well known that the reverse biasing of detectors often improves the external quantum efficiency by increasing the carrier collection efficiency within the detector (internal quantum efficiency). As mentioned previously, it was found that reverse biasing the Schottky diodes often caused contact breakdown, resulting in the transformation from a Schottky contact to an ohmic. Therefore, no tests were made under reverse bias.

The short circuit current was measured on a Keithly 610B electrometer. The external quantum efficiency was then determined by comparing the detector short circuit current to the short circuit current produced by a calibrated silicon solar cell put in place of the

UV detector and held behind a 1 mm diameter pinhole. The relationship for external quantum efficiency is

$$\eta = \eta_{sc} \frac{I_D/A_D}{I_{sc}/A_{sc}} \quad (3)$$

where A_D is the area of the UV detector, η and I_{sc} are the external quantum efficiency and short circuit current of the solar cell and A_{sc} is the area of the pinhole ($D=1$ mm). A tabulation of values measured at the UV detector response peak is given below.

Sample	x-value	Spectral Peak (nm)	External Quantum	
			Typical	Maximum
GaN 35	0	352	2	5.5
AlGaIn 43	0.04→0.07	340	0.2	0.5
AlGaIn 42	0.12→0.22	260-280	?	?

The signal-to-noise ratio for the measurements on AlGaIn 42 was too low to obtain any meaningful values ($I_D < .1$ nA). It was possible, however, to determine that the spectral peak for the detectors was in the range of 260-280 nm.

One disappointing aspect of these measurements was the low quantum efficiency of AlGaIn 43. As shown above, the open circuit voltage of some detectors from AlGaIn 43 matched those from GaN 35. However, before accurate efficiency measurements were made, the quality of the Schottky contact degraded appreciably due to a large increase in current leakage. The cause of this added leakage is unknown, however, it is hypothesized that probing of the Schottky contacts caused localized areas to convert to ohmic contacts. This effect must be studied further.

The internal quantum efficiency of a detector is the ratio of the number of carriers collected in the detector versus the number of photons entering into the absorbing region. It is, therefore, independent of contact configuration or transparency, but is very dependent on material quality and the integrity of the Schottky contact.

The internal quantum efficiency can be found by dividing the external quantum efficiency by the fraction of incident light which is transmitted into the bulk AlGaIn. The amount transmitted is the total incident power minus the sum of the light reflected

plus the light absorbed in the gold contact. Using the theory developed by Heavens¹⁷ which employs the complex index of refraction, $n + ik$, the reflection of light at 3000Å from a 150Å layer of gold ($n = 1.41$, $k = 1.8$) on GaN ($n = 2.03$, $K = .48$) is approximately 35 percent. The absorption suffered by light at 3000Å wavelength as it travels through 150Å of gold is 68 percent. Therefore, only 21 percent of the light actually enters the absorbing active region. The internal quantum efficiency is five times higher than the external quantum efficiency. In a good detector, however, the internal quantum efficiency should be over 90 percent which is much higher than any device tested. Therefore, there is a great deal of room for improvement in the AlGaIn Schottky detectors. Some possible areas of future research are discussed in the next section.

Sample AlGaIn 42, having x -values between 0.11 and 0.22, had its spectral response peak at 267 nanometers (4.64 eV) which is below the long wavelength cut-off due to the ozone in the stratosphere. Because of excessive leakage currents, the sensitivity of this sensor was very low, and not much can be said with accuracy about the shape of its spectral response curve. However the response curves of both GaN 35 and AlGaIn 43, both of which peak in the near ultraviolet, fall off nearly two orders of magnitude in about 0.3 eV on the long wavelength side of the peak and it is expected that material with shorter wavelength response should behave similarly. Also the composition of AlGaIn 42 varied from an X -value of 0.11 to 0.22. Thus the slope on the response curve and the long wavelength tail may be due to the lack of uniformity in the aluminum concentration. The production of more uniform material could be achieved by such means as rotating the substrate during growth and better flow control of reactant gases.

¹⁷ O.S. Heavens, "Physics of Thin Films" (1979).

Section 6

Discussion of Results and Areas of Future Investigation

Attempts to grow epilayers of the $\text{Al}_x\text{Ga}_{1-x}\text{N}$ system with a resistivity high enough to make Schottky barrier diodes directly on the material have been unsuccessful. The attempts have included zinc doping up to 10 percent Zn and growing material with aluminum concentrations up to $x = .22$. The causes of the low resistivity are (a) native nitrogen vacancies and (b) silicon contamination from the reactor nozzle. However, it has been possible to form Schottky barrier diodes on GaN and $\text{Al}_x\text{Ga}_{1-x}\text{N}$ by ion implantation to a depth of 1 micron with beryllium. C-V measurements indicate a carrier concentration of 10^{17}cm^{-3} . This was very encouraging because it made possible the spectral response measurements on these epilayers. The peak of the spectral response for GaN was 351 nm. For a Schottky diode on $\text{Al}_x\text{Ga}_{1-x}\text{N}$ with a reported composition range of x from 0.04 to 0.07 the peak occurred at 343 nm, and for material with an x value that ranged from 0.11 to 0.22 it was at 267 nm. These values are approximately what is expected on the basis of composition from Vegard's law.

The Schottky detectors fabricated from the implanted layers were operated in both the open circuit voltage mode and short circuit current mode. Attempts at operating the diodes under reverse bias were not successful because the devices were often destroyed when the contact changed from a Schottky to an ohmic characteristic. We believe that this was caused by localized areas of alloying of the gold contact to the AlGa N due to heat generated by leakage current through crystal defect.

Several factors related to both the materials and the processing limited the performance of the AlGa N UV detectors during this initial investigation, but there are a number of specific steps which can be taken to improve these results. As is the case with most simple electronic devices, improvements in the material quality will produce the greatest increase in device performances.

Areas of materials development which have been identified for future improvement are:

- Improvements in the MO-CVD growth system. The growth of controlled compositions of $\text{Al}_x\text{Ga}_{1-x}\text{N}$ will require the use of mass flow controllers in the gas lines. These have already been purchased but have not yet been installed. Substrate rotation in the MO-CVD system will be required to assure layer thickness and

compositional uniformity. Increased leak tightness should be used in order to guard against the reaction of oxygen with the aluminum during growth.

- Study of growth materials. A study of the materials and procedures directly relating to the growth must be undertaken. This includes the use of substrates and gases from a number of vendors for the purpose of determining those that yield the best results.
- Increased production of high quality layers. During this initial investigation, many of the samples grown by MO-CVD were not generally of device quality and the great lack of uniformity on individual wafers prevented accurate characterization. By including the improvements mentioned above, large areas of high quality material will be available for device fabrication. These layers must be single crystal, low defect density and compositionally uniform in order to produce solar blind UV detectors.
- Growth of AlGa_N by molecular beam epitaxy. Molecular beam epitaxy (MBE) is the growth technique with the greatest potential for precise control over composition and uniformity of epitaxial layers. This technique has not been investigated for the epitaxial growth of AlGa_N. However, since the growth kinetics of MBE are different from those of MO-CVD, defect formation and the compensation mechanism may well be different for the two techniques. Therefore, we should grow AlGa_N epilayers by MBE and compare the electrical and optical parameters of material grown by this technique with those of material grown by MO-CVD.

Because of problems with the current MO-CVD growth system, few single crystal AlGa_N epilayers were available for device processing. With the above improvements, more samples of higher quality are available, and it is expected that further improvements will result from more extensive investigation of the devices in the fabrication procedure. Those areas which should be investigated as far as device processing is concerned include:

- Ion Implantation. We have already demonstrated that material can be compensated by the implantation of acceptor atoms (beryllium), permitting the formation of Schottky barriers. Saxena et al.¹⁸, have reported making Schottky barriers on Ga_N epilayers ion implanted with 60 KeV N⁺. The carrier concentration in the nitrogen implanted layer was about 10^{16}cm^{-3} . The reduction in this case was due to the filling in of the native nitrogen vacancies responsible for the high carrier concentration. A more comprehensive study of implantation of both beryllium and nitrogen should be carried out in a future program. This study should

¹⁸ A.N. Saxena, L.R. Weisberg, W.B. Mann, F.J. Schima, Int. J. Appl. Rad. and Isot. 26, 33 (1975).

include variations in implant energies and dosages as well as anneal times and temperatures.

- **Schottky Contacts.** One cause of low device performance was the excess leakage current across the Schottky barrier. It was noted that the amount of leakage often increased with time and testing. It is therefore suspected that the gold contact began to alloy with the gallium from the decomposing AlGaIn to become ohmic. This could occur at defect centers where the current density, and thus the temperature, was high; a problem which could be eliminated by improved layers and metals. Possible metals include chromium, titanium, and platinum. The choice of contact metal is also dependent on transparency, stability and fabrication ease.

A more thorough investigation of cleaning procedures and device handling will be very useful in the determination of causes of device degradation and failure.

- **Improved Configuration for Detectors.** Because this was a preliminary investigation, no effort was made to develop the optimum configuration for the detection. In future work, much use can be made of an already existing technology in the design of the device structure. Insulating oxide coatings and bonding pads should be added in order to improve the stability of the contact and eliminate degradation and shadowing during probing. Guard rings around the contact dot should be added to decrease surface leakage current and increase the signal to noise.
- **Addition of Antireflection Coating.** Once an optimized detector has been fabricated, its efficiency can be further enhanced by antireflection coating the Schottky contact. The antireflective coating will not only provide higher efficiency in the UV, but can be designed to make the detector more solar blind by discriminating against the visible spectrum.

Section 7 Conclusions

In the course of this investigation, our experiments have shown that:

- Single crystal GaN and AlGa_N can be grown epitaxially on sapphire by MO-CVD.
- Resistivities of as grown GaN and Al_xGa_{1-x}N epilayers so far observed have been 1 to 2 orders of magnitude too low for Schottky barrier formation, even with Zn doping up to 10% and x-values up to .22.
- Schottky barriers may be formed on GaN and AlGa_N epilayers after compensation of the AlGa_N surface by acceptor ion implantation.
- Aluminum content (x-value) controls the spectral response of Schottky barriers on ion implanted Al_xGa_{1-x}N as predicted by Vegard's Law.
- Fabrication of UV photo diodes from Al_xGa_{1-x}N materials has been demonstrated.
- Detectors were fabricated with peak sensitivities in the 3.53 eV to 4.64 eV range.

In the preliminary investigation, we demonstrated the feasibility of AlGa_N for UV detectors. Already this material has shown promise as the basis for high quality, solid-state UV detectors. With improvements in material quality and uniformity, in carrier reduction techniques, and in Schottky barrier formation, we believe this material can be used to produce stable, highly sensitive and solar blind UV detectors.

References

1. M. Gershenzon, Annual Technical Progress Report, "Evaluation of Gallium Nitride for Active Microwave Devices." ONR N00014-75-C-0295, Sept. 1978 (AD A064299).
2. M. Gershenzon, Annual Technical Progress Report, "Evaluation of Gallium Nitride for Active Microwave Devices," ONR N00014-75-C-0295, Sept. 1979 (AD A079319).
3. M. Illegems and H.C. Montgomery, J. Phys. Chem Solids 34, 885 (1973).
4. J.I. Pankove, J.E. Berkeyheiser and E.A. Miller, J. Appl. Phys. 45, 1280 (1974) (and reference appended).
5. G. Jacob, R. Madar and J. Hallais, Mater. Res. Bull. 11, 445 (1976).
6. R. Madar, G. Jacob, J. Hallais and R. Fruchart, J. Cryst. Growth 31, 197 (1975).
7. G. Jacob, Acta Electron. 21, 159 (1978).
8. G. Jacob, M. Boulow and M. Furtado, J. Cryst. Growth 42, 136 (1977).
9. R. Madar, D. Michel, G. Jacob and M. Boulow, J. Cryst. Growth 40, 239 (1977).
10. G. Jacob, M. Boulow, M. Furtado and D. Bois, J. Electron. Mater. 7, 499 (1978).
11. J. Hagen, R.D. Metcalfe, D. Wickenden and W. Clark, J. Phys. C. 11, L143 (1978).
12. B. Baranov and L. Daeweritz, Phys. Status Solidi A 38, K111 (1976).
13. B. Baranov, L. Daeweritz, V.B. Gutan, G. Jungk, H. Neumann and H. Raidt, Phys. Status SolidiA 49, 629 (1978).
14. R.A. Logan and C.D. Thurmond, J. Electrochem. Soc. 119, 1727 (1972).
15. L.B. Ta, Ph.D. Thesis, University of Southern California (1981).

16. L. Anne, Ph.D. Thesis, University of Southern California (1979).
17. O.S. Heavens, "Physics of Thin Films" (1979).
18. A.N. Saxena, L.R. Weisberg, W.B. Mann, F.J. Schima, Int. J. Appl. Rad. and Isot. 26, 33 (1975).